Supplemental

Title: Spatial estimates of soil moisture for understanding ecological potential and risk: a case study for arid and semi-arid ecosystems

Authors: Michael S. O'Donnell and Daniel J. Manier

Contents

S1. Data sources and descriptions

We used numerous spatial datasets for generating, evaluating, and comparing soil-climate products. Details of producer, description, source scale/resolution, geographic extent, ground date, and download date are described in Table S1. The analyses described in the manuscript used various data for different tasks, and we link the 'Category' column (Table S1) with each analysis stage to describe data dependencies (Figure S1). We derived several terrain indices from the digital elevation model, which are described below. All analyses and derived data used a Conical Albers Equal Area with standard parallels appropriate for the contiguous United States and a 1984 World Geodetic System datum. We used a resampling algorithm of nearest neighbor (discrete data) or bilinear (continuous data) when reprojecting raster surfaces.

Table S1. Description of data sources used in our implementation of the Newhall simulation modeling framework applied to western United States (U.S.) from 1981 to 2010. Each dataset description includes important and relevant information on scale/resolution, geographic extent, ground dates, and access dates.

Category	Producer	Description	Source scale/ resolution	Geographic extent	Ground date	Access date
Climate gridded	Prism Climate Group [1]	Monthly temperature and precipitation (mm)	800 m	Contiguous United States	30-year normal; 1980-2010	20 Dec. 2017
Soil-climate monitoring network	U.S. Department of Agriculture [2]	Soil climate analysis network (SCAN) monitors soil moisture and temperature (°C) at several depths, as well as air temperature, relative humidity, solar radiation, wind speed and direction, liquid precipitation, and barometric pressure. Soil temperature and soil moisture measurements are observed at the depths of 5, 10, 20, 50, and 100 cm.	NA[1]	Contiguous United States	1988 – 2020	9 Apr. 2020
	Dorigo*, et al.* [3]	International soil moisture network (ISMN)		Global	hourly measurements for years stations exist and at multiple depths	7 Jul. 2022
Climate stations	Arguez*, et al.* [4]	Climate stations defining 1981 – 2010 U.S. climate normal conditions available from the National Climate Data Center	NA	Contiguous United States	monthly normal (1981 – 2010),	24 Jan. 2020
Snow[2]	National Operational Hydrologic Remote Sensing Center [5]	Snowpack properties, such as depth and snow water equivalent (SWE), from the NOAA National Weather Service's National Operational Hydrologic Remote Sensing Center (NOHRSC) snow data assimilation system (SNODAS)	1 km	Contiguous United States	daily, Oct. 2003 – Dec. 2019	24 Mar. 2020

Category	Producer	Description	Source scale/ resolution	Geographic extent	Ground date	Access date
Polaris soils[3]	Chaney, *et al.* [6],Chaney, *et al.* [7]	Soil properties defined using high-resolution environmental data and machine learning algorithm (Disaggregation and Harmonization of Soil Map Units Through Resampled Classification trees [DSMART]). We used soil properties: alpha, n, $theta_r$, $theta_s$, and organic matter at multiple depths (0 – 5 cm, 5 – 15 cm, 15 – 30 cm, 30 – 60 cm, 60 – 100 cm, 100 – 200 cm) and median percentile (p50).	30 m	Contiguous United States	NA[3]	6 Mar. 2017
USDA[4] soils	Soil Survey Staff [8]	Gridded national soil survey database (gNATSGO) is a composite of the Soil Survey Geographic Database (SSURGO), State Soil Geographic Database (STATSGO2), and Raster Soil Survey Databases (RSS). At a given pixel, the most accurate (SSURGO) to least accurate (STATSGO2) spatial data are used to create the gNATSGO composite.	30 m; 1:12,000 to 1:63,360	Contiguous United States	NA	5 Apr. 2021
Derived USDA soils	Maestas, *et al.* [9]	Data of soil temperature and moisture regimes with estimates of resilience and resistance to help land managers determine how pixels are likely to respond to disturbances and management. These products were derived from the Natural Resources Conservation Service of U.S. Department of Agriculture data (Soil Survey Geographic Database [pSSURGO]).	30 m	Greater sage-grouse range (*Centrocercus urophasianus*)	NA	7 Apr. 2017
Elevation	U.S. Geological Survey [10]	3D elevation program, 1/3 arc-second seamless product	10 m	Contiguous United States	Varies	4 Apr. 2018

Category	Producer	Description	Source scale/ resolution	Geographic extent	Ground date	Access date
Land cover type	Yang, *et al.* [11]	The National land cover database (NLCD) provides nationwide data on land cover with a 16-class legend based on a modified Anderson Level II classification system.	30 m	Contiguous United States	2016	28 May 2019
Vegetation cover type	U.S. Geological Survey [12]	LANDFIRE Existing Vegetation Type layer version 2.0.0	30 m	Contiguous United States	2016	30 Jan. 2021
Sagebrush cover	Rigge, *et al.* [13],Xian, *et al.* [14]	Sagebrush fractional shrub components, including sagebrush	30 m	Sagebrush biome	2016	15 May 2019
Fire (burned pixels)	Hawbaker, *et al.* [15]	Landsat burned area essential climate variable products for the conterminous United States (1984 - 2016)	30 m	Contiguous United States	1984 – 2016	25 Feb. 2021
Annual grasses	Maestas, *et al.* [16]	Annual herbaceous cover across rangelands of the sagebrush biome	30 m	Sagebrush biome	2016 – 2018	24 Feb. 2021
Watershed boundaries	U.S. Geological Survey [17]	National hydrologic data high resolution	1:24,000	Contiguous United States	NA	20 Dec. 2017
Tree canopy cover	U.S. Geological Survey [18]	Tree canopy cover for analytical processing	30 m	Contiguous United States	2016	5 Mar. 2021
Hydrology	U.S. Geological Survey [17]	National hydrography dataset high resolution (NHDH)	1:24,000	Contiguous United States	2016	20 Dec. 2017

[1]NA: not available or varies due to extensive sampling during decadal surveys.

[2]Solid snow precipitation (product identifier 1025SlL01): units=kg/m^2, scale=10; Non-snow (liquid) precipitation (product identifier 11025SlL00): units=kg/m^2, scale=10.

[3]*theta_s* represents saturated soil water content (m^3/m^3); *theta_r* represents residual soil water content (m^3/m^3); *n* represents the measure of the pore size distribution (van Genuchten; unitless); *alpha* represents the scale parameter inversely proportional to mean pore diameter (van Genuchten) (log10(kPa-1)); *om* represent organic matter (log10(%)).

[4]U.S. Department of Agriculture Natural Resources Conservation Service

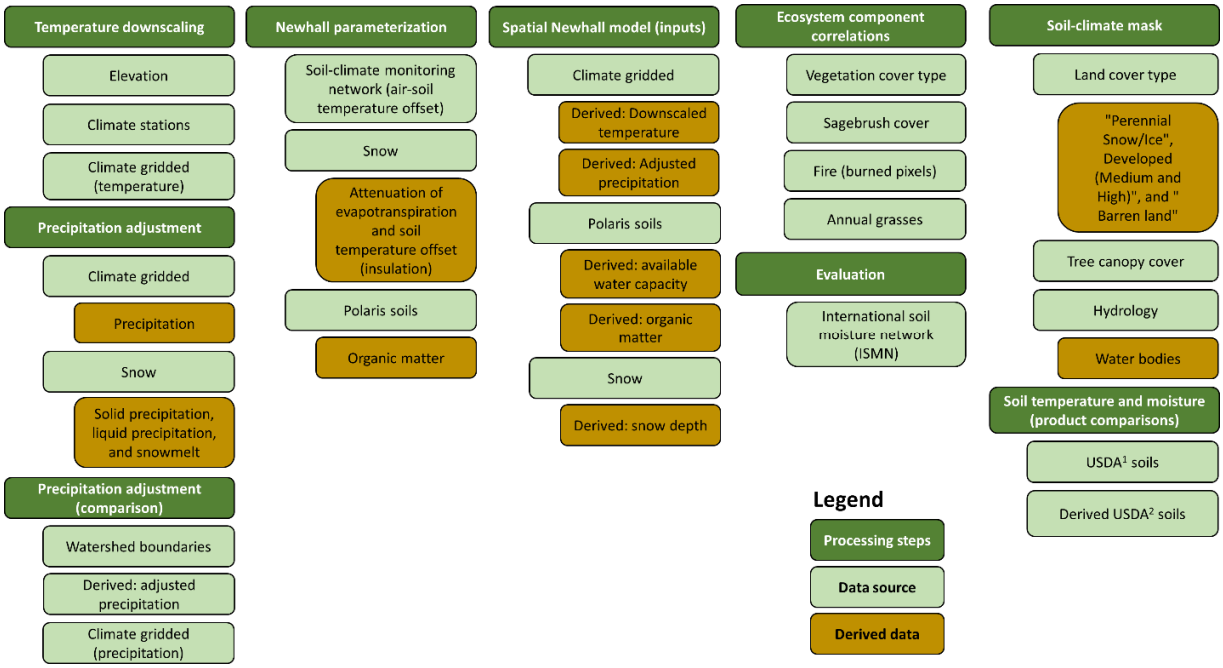

Figure S1. Processing steps describing our analyses to implement the Newhall spatial model rely on numerous data inputs and interim derived data products. Details on data inputs are described in Table S1. [1]USDA: U.S. Department of Agriculture, Natural Resources Conservation Service is responsible for mapping and disseminating soil data. [2]Derived USDA: Data of soil temperature and moisture regimes with estimates of resilience and resistance.

Snow data assimilation system (SNODAS): These data provide numerous estimates of snow cover, depth, snow water equivalent (SWE) and numerous indices to support hydrologic modeling. One study [19] located in Colorado, USA observed the models performed well in forested areas (accounted for 72% of variance in snow depth and 77% of snow water equivalency [SWE]), but performed poorly in alpine areas (16% of variance in snow depth and 30% of variance of SWE). Additional studies evaluating SNODAS also demonstrated similar biases and several methods for potentially correcting for those biases [20-22].

Polaris soils data: The Polaris data [6,7] are a probabilistic version of the U.S. Department of Agriculture (USDA) Natural Resources Conservation Service (NRCS) soil data. A machine learning algorithm called disaggregation and harmonization of soil map units through resampled classification trees (DSMART) was used to define soil series (classification level in the USDA soil taxonomy) within USDA map units (soil components). With these products and high-resolution environmental data, Chaney, Minasny, Herman, Nauman, Brungard, Morgan, McBratney, Wood and Yimam [6] modeled soil properties (soil horizon) using various methods. Although we relied on Polaris soils [6,7] specifically developed in the contiguous United States to estimate available water capacity (AWC), an alternative global soils product exists (SoilGrids250m) [23], which others have then derived AWC (https://data.isric.org/geonetwork/srv/api/records/e33e75c0-d9ab-46b5-a915-cb344345099c,

accessed 7/28/2022). Therefore, AWC derived from SoilGrids250m may be useful for applications outside the United States.

Polaris soils caveats: We encountered two conditions where Polaris soil properties data [6] contained suspect values. First, we discovered minute discernable differences for 5 – 15 cm depth of $theta_s$ and $theta_r$ using the median product (p50). As a result, calculating AWC resulted in values of zero for most pixels at this depth within our study area. The AWC for all other depths approximated near-equal differences at individual pixels, where each previous depth was approximately half the value of the next incremental depth—except for the depth 5 – 15 cm. Therefore, we averaged the AWC depths of 0 – 5 cm and 15 – 30 cm to define AWC at 5 – 15 cm depth. Second, few pixels (3,564,010 pixels) were assigned no data values in Polaris data (Figure S2). We used Esri® ArcGIS™ [24] Nibble™ geoprocessing tool in the Spatial Analyst™ extension to replace these no data values within the AWC using a pixel value from its nearest neighbor.

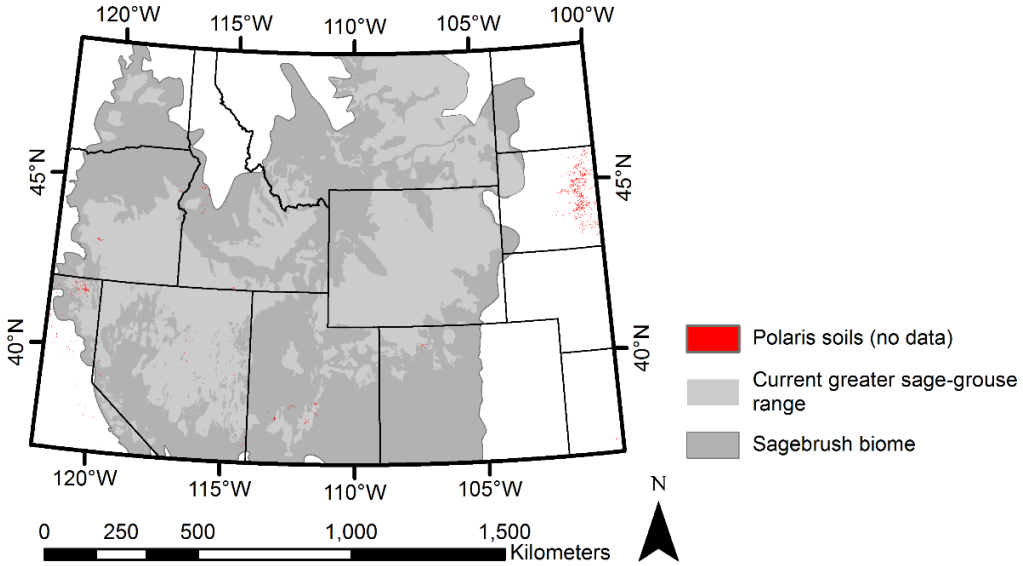

Figure S2. Distribution of no data occurrence within available water capacity (AWC). We derived AWC from Polaris soils data [6,7] and replaced no data using data from the nearest pixel. The AWC informed the creation of soil-climate data products produced from implementing the Newhall simulation modeling framework applied to the western United States from 1981 to 2010. Users of the soil-climate products may decide to use the mask of no data presented here to omit pixels from any future analyses.

United States Department of Agriculture (USDA) Natural Resources Conservation Service (NRCS) soil data: Soil temperature and moisture regime classifications are defined within soil data developed by the U.S. Department of Agriculture (USDA) Natural Resources Conservation Service (NRCS). The USDA gridded product known as gSSURGO represents the spatial and aspatial products of SSURGO (CONUS survey [contiguous United States] unit map scale of 1:12,000 to 1:63,360). The USDA also developed a gridded national soil survey database

(gNATSGO) of the soil survey geographic database (SSURGO), state soil geographic database (STATSGO2; CONUS survey unit map scale of 1:250,000), and raster soil survey databases (RSS). The gNATSGO was developed to address unmapped areas of gSSURGO by infilling with STATSGO2. These soils data (all products) reflect spatial and aspatial information organized as a relational database with one-to-many and many-to-many joins. The map unit polygons/pixels of the soil data products represent the soil survey unit, which contains one to four predominant soil components, aspatially expressed as a percentage of a map unit's area. Soil properties for each component (aspatial) also provide information about temperature and moisture regimes by soil depth (a one-to-many relationship between the component and component horizon data). We describe NRCS data products as they were used in part to develop Polaris soils data. We also used the NRCS soil temperature and moisture classifications to compare with our soil temperature and moisture classifications (defined from our soil-climate analyses).

Hydrologically corrected digital elevation model: We created a 10-meter digital elevation model (DEM) of the western United States by mosaicking elevation tiles [10]. The DEM was hydrologically corrected to reduce the number of elevation anomalies using the optimized pit removal software [25; v. 1.5.1]. Peaks and troughs of two to five meters are rare within 10-m DEMs and generally reflect errors [26]. Correcting this noise improves flow accumulation analyses, which we used in different terrain-derived indices. We used these corrected results for all derived terrain indices described below.

Heat load index: The heat load index (HLI) identifies the potential annual direct incident radiation suitable for our latitudes of 30 – 60 degrees North [regression equation three [R2 = 0.983]; 27]. The equation includes latitude, slope, and aspect, where the coolest slopes occur on northeastern aspects and the warmest slopes on southwestern aspects (northern hemisphere). The values can range from 0 (little to no variation in the terrain and therefore coolest) to 1 (significant variation and therefore hottest), but most natural terrain have values distributed below 0.5. The index does not account for cloud cover, regional differences in the atmospheric coefficient, or shading due to topography.

Vector ruggedness measure: We developed a vector ruggedness measure (VRM), defined by Sappington*, et al.* [28], using a radius of 30 m to capture small-scale terrain features. The VRM is like other forms of calculating terrain ruggedness, but it incorporates slope and aspect, unlike other methods.

S2. Description of Python implementation of Newhall simulation model

We developed open-source software (*spatial_nsm*) to accomplish most analyses using Python™ libraries, including primarily *gdal* [29], *geopandas* [30], *numpy* [31], pandas [32], *rasterio* [33], *scikit-learn* [34], *scipy* [35], *shapely* [36], and *statsmodels* [37]. More information about the software and its use is provided in the software repository (see main manuscript; [38]).

- Python implementation was cross-referenced to *jNSM* 1.6.1.
- We annotated Newhall simulation code.
- We removed redundant code by using functions.

- We used a function for calculating the Thornthwaite-Mathers-Seller PET equation, allowing the use of different evapotranspiration methods.
- We added *jNSM* 1.6.1 line references for quality assurance.
- We provided support for aspatial and spatial applications.
- We provided support for monthly air-soil temperature offsets.
- We added options to include organic matter to inform temperature classification, the proportion of days with snow cover >12 cm, and the ability to offset soil temperature at 50 cm due to insulating factors of snow. CAUTION: air-soil temperature offset informed from SCAN includes winter months, but these do not occur in areas where snow persists.
- Spatial component of the software can run on a single machine using all available cores and memory or on a high-performance computing cluster.
- Spatial and aspatial unit tests were provided.
- Detailed logging to a text file for many stages of the model is available for quality assurance. However, logging should not be enabled for spatial models because there is too much information to track at each pixel.
- We added an alternative soil temperature and moisture regime classification tree and modified existing classification methods implemented within *jNSM* 1.6.1 to decrease the number of instances pixels not classified. The alternative classification is described in sections S9 and S10.

S3. Modeling and high-performance computing

Data pre-processing and post-processing were executed on a workstation with two Intel® Xeon® computer processing units (CPU; E5-2667 v4 at 3.2 gigahertz [GHz] with a total of 32 logical processors) and 64 gigabytes (GB) memory using a Microsoft® operating system. Pre-analysis required approximately 320 wall clock hours, recognizing that we did not document runtime for all steps. The spatial Newhall simulation model (NSM) was executed on a high-performance computing cluster [39] with 232 Cray® XC-50 compute nodes, each with a dual 2.4 GHz Xeon CPU and 192 GB memory. A 2.4 petabyte (PB) Lustre storage with 35 GB/s peak read/write speeds served as storage (~5 terabytes [TB] of storage required for data input and a similar amount for output). The cluster used a simple Linux utility resource manager (SLURM) for scheduling jobs. Each submitted SLURM job executed the model using map tiles (data decomposition) coinciding with the western United States. Using our method for distributing jobs on the cluster, we used 23 compute nodes, each executing the NSM for multiple tiles in parallel, resulting in ~850 wall clock hours (completed in ~2 days). Post-analysis required ~90 hours, including merging tiled soil-climate data products and running trend estimates (we did not document runtime for all steps).

S4. Data used for Newhall simulation

We used climate stations defining 1981 – 2010 climate normal conditions available from the National Climate Data Center [1507 stations; 4] for downscaling gridded PRISM temperatures [Figure S3a; 1]. Soil network stations from the Soil Climate Analysis Network (SCAN) were used to define 1988 – 2020 climate normal conditions available from the Natural Resources

Conservation Service, National Water and Climate Center [Figure S3b; 61 stations; 2]. The SCAN data were used to inform monthly air-soil temperature offsets (Figure S4), which we adjusted and used due to a lack of representative data (Table S2) to more closely reflect the default of 2.5°C used in other research [40,41]. During winter conditions when snow cover was present at a depth ≥12 cm for >50% of the days within a month, we adjusted soil temperatures based on literature [Table S2; 42].

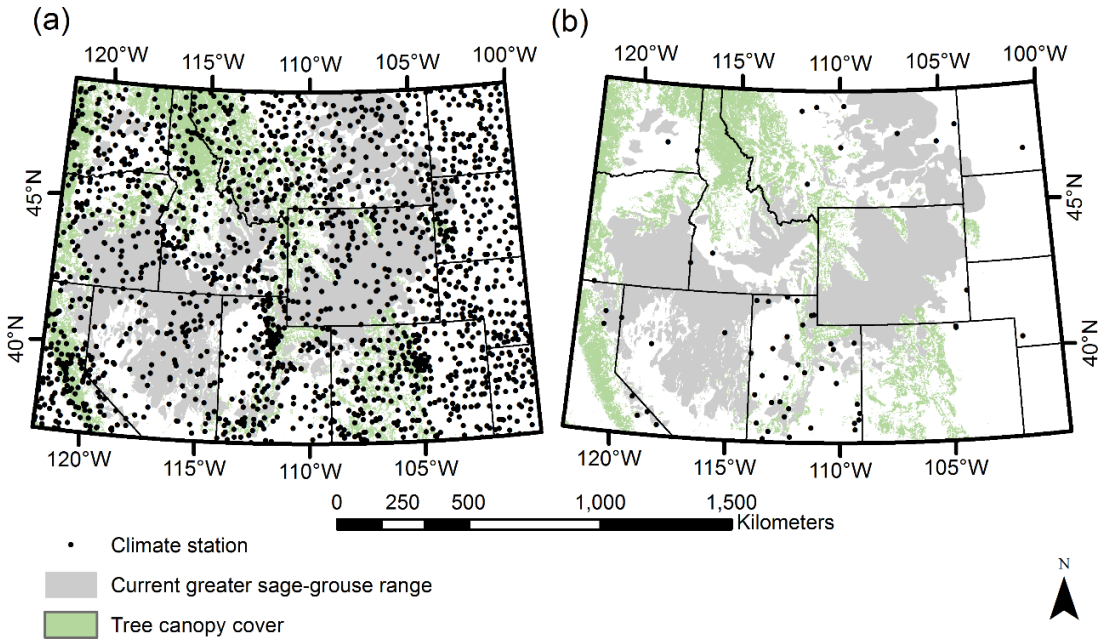

Figure S3. Spatial locations of climate and soil sensor data used our implementation of the Newhall simulation modeling framework applied to the western United States from 1981 to 2010. Climate stations (a) defining 1981 – 2010 U.S. climate normal conditions available from the National Climate Data Center [1,507 stations; 4] and Soil Climate Analysis Network (SCAN; b) stations defining 1988 – 2020 climate normal conditions available from the Natural Resources Conservation Service, National Water and Climate Center [61 stations; 2]. The greater sage-grouse range (*Centrocercus urophasianus*) coincides with the sagebrush biome.

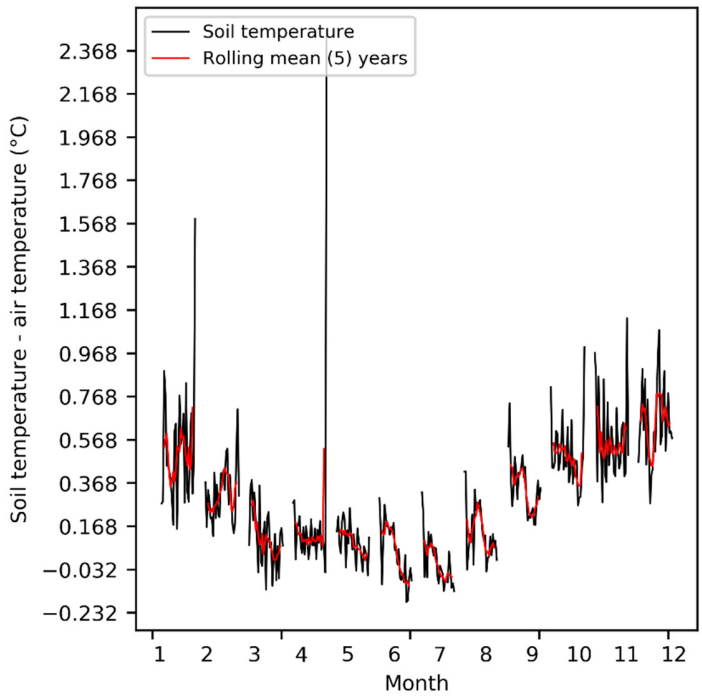

Figure S4. Results from investigating soil sensor data used our implementation of the Newhall simulation modeling framework applied to the western United States from 1981 to 2010. Monthly mean soil temperature extracted from the Soil Climate Analysis Network (SCAN) stations defining 1988 – 2020 climate normal conditions available from the Natural Resources Conservation Service, National Water and Climate Center [61 stations; 2]. The black line captures the monthly mean by year, and the red line captures a 5-month rolling mean where months were averaged across 5-years.

Table S2. Monthly mean soil-air temperature offset (soil temperature at 50 and 100 cm relative to air temperature [°C]) based on the Soil Climate Analysis Network (SCAN) stations defining 1988 – 2020 climate normal conditions within the western United States (data from Natural Resources Conservation Service, National Water and Climate Center; 61 stations).

Month	Mean temp. (°C) offset at 50 cm (20 in)	Mean temp. (°C) offset at 100 cm (40 in)	Mean temp. (°C) offset at 50 cm (20 in)	Mean temp. (°C) offset: NSM input
Jan	0.57	0.81	1	2
Feb	0.35	0.52	0	2
Mar	0.06	0.12	0	1
Apr	0.14	0.07	0	0
May	0.05	-0.10	0	0
Jun	-0.04	-0.30	0	-2
Jul	-0.06	-0.34	0	-2
Aug	0.09	-0.11	0	0
Sep	0.28	0.24	0	0
Oct	0.46	0.61	1	1
Nov	0.55	0.82	1	2

Month	Mean temp. (°C) offset at 50 cm (20 in)	Mean temp. (°C) offset at 100 cm (40 in)	Mean temp. (°C) offset at 50 cm (20 in)	Mean temp. (°C) offset: NSM input
Dec	0.67	0.96	1	2

Based on data from 574 snowpack telemetry stations (SNOTEL; U.S. Department of Agriculture Natural Resources Conservation Services network) spanning the western United States, snowpacks resulted in warmer soils compared to air temperature during the winter where mean soil temperature was 1.3°C warmer than ambient temperature at 50 cm. However, mean interannual and intersite soil temperatures ranged between 1°C and 6°C warmer than air temperature where variability was due to early snowpack conditions [43]. Notably, most SNOTEL stations do not exist in the sagebrush steppe, and these results may not reflect all conditions within the western United States. When snow cover is thin or absent in winter, the difference between soil and air temperature is minimal [44,45]. During the spring, when snowmelt occurs, the ground surface temperature is several degrees lower than the air temperature [46].

Smith, Newhall, Robinson and Swanson [42] described results of a study [47] where soil temperature and air temperature on bare and snow-covered sites at Leningrad, Russia (now Saint Petersburg) were observed. These results captured the following information: 1) April/November soil ~0.5°C warmer at snow-covered sites, where Apr. had 75 cm snow and Nov. had 12 cm snow; 2) December soil was ~2°C warmer at snow-covered sites with ~25 cm snow depth; 3) March soil ~3°C warmer at snow-covered sites with ~87 cm snow depth; and 4) January/February soil was ~4.5°C warmer at snow-covered sites with ~62 and ~87 cm snow depth respectively. Based on the various studies, we estimated air-soil temperature offsets (Table S3) to more accurately capture the effects of snow cover on soil temperatures.

Table S3. Adjustments were made within the Newhall simulation model software (*nsm_spatial*) for soil temperature at 50 cm when the proportion of days (>50%) with snow cover and a depth ≥12 cm occur for a given month and pixel. Offsets reflected estimates observed in the Northern hemisphere [42].

Month	Mean temp. offset (°C) at 50 cm	Snow depth (cm)	Air temp. (°F, °C)	Mean temp. offset (°C) at 50 cm: NSM input
Jan	4.5	37	16, -8.8	5
Feb	5	57	16, -8.8	5
Mar	2	60	22.5, -5.3	2
Apr	0.3	32	36, 2.2	0
May	0	--	--	0
Jun	0	--	--	0
Jul	0	--	--	0
Aug	0	--	--	0
Sep	0	--	--	0
Oct	0	--	--	0
Nov	0.8	7	28.5, -1.9	2[1]
Dec	3	17	23, -5	3

[1]We adjusted the value to 2°C because our offsets only apply with >12 cm of snow depth versus 7 cm in the data.

S5. Temperature downscaling

We use random forest machine learning to downscale temperature from 800-meter resolution to 30-meters. Our approach included multiple candidate covariates and number of trees. Specifying

more trees typically results in better model performance but requires longer computation time. We also specified a parameter to tag every observation used in the different trees, allowing the model to differentiate between validation and training observations (akin to leaving one out). We calculated the R^2 score (coefficient of determination) to measure how well a model performs relative to a mean of the target values, where $R^2=1$ indicates perfect predictions, 0 indicates the model does not perform better than using the mean of the data, and values <0 indicate extremely poor models. We used pixel values for any PRISM data cells colder than the global minimum

Numerous performance measures exist for evaluating machine learning results. We discuss several of these here, defined in Vandeput [48] and further explained in the literature [e.g., 49,50]. Mean absolute error (MAE) is the average of all data points' residuals, describing the magnitude of difference (absolute) between observed and expected (i.e., residuals/errors) while giving less weight to outliers. Mean absolute percentage error (MAPE) is similar to MAE but normalized by the observation value, where the absolute error is calculated as a percentage for each error before being averaged. If the observation has a value of zero, the metric cannot be calculated due to division by zero. Mean squared error (MSE) averages the squares of residual difference and represents the combined measurement of bias and variance of estimated values. Because the MSE grows quadratically, data outliers will contribute to a much higher total error than MAE. Root mean square error (RMSE) is the square root of the MSE and can result in a relatively high weight when large errors are present. The RMSE is always ≥MAE, and the greater the difference, the greater the variance in the individual sample errors. The mean percentage error (MPE) is similar to MAPE but does not calculate the absolute value. Table S4 provides results of downscaling temperature for top models, where methods are described in the main manuscript.

Table S4. Model performance of downscaling monthly mean temperature using 1981 – 2010 United States climate normal conditions available from the National Climate Data Center [1,507 stations; 4]. Candidate covariates of the top two models included the parameter-elevation regressions on independent slopes model [PRISM; 1981 – 2010 normals; ptmean; 1], heat load index (hli), vector ruggedness measure (vrm), and digital elevation model (dem). Performance metrics included mean absolute error (MAE), mean absolute percentage error (MAPE), mean squared error (MSE), root mean square error (RMSE), percent accuracy (100 - MAPE), cross-validation R^2, and MSE. We evaluated two different models, and we selected model b (sta_mean ~ "ptmean", "hli", "dem", "vrm") as it performed consistently better.

		Variable Importance					Model performance metrics						
Month	**Model**	**ptmean**	**hli**	**dem**	**vrm**	**R^2**	**MAE**	**MAPE**	**MSE**	**RMSE**	**Percent accuracy**	**Cross-validation R^2**	**Cross-validation MSE**
Jan	a	0.97	0.02	0.02		0.95	0.65	0.24	0.78	0.88	99.76	0.33	11.18
	b	0.97	0.01	0.01	0.01	0.95	0.64	0.24	0.77	0.87	99.76	0.35	10.86
Feb	a	0.97	0.01	0.02		0.96	0.62	0.23	0.65	0.81	99.77	0.37	10.37
	b	0.97	0.01	0.01	0.01	0.96	0.62	0.23	0.64	0.8	99.77	0.39	10.12
Mar	a	0.96	0.02	0.02		0.96	0.56	0.2	0.51	0.72	99.8	0.42	6.89
	b	0.96	0.01	0.02	0.01	0.957	0.55	0.2	0.51	0.71	99.8	0.43	6.81
Apr	a	0.95	0.02	0.03		0.94	0.52	0.18	0.46	0.68	99.82	0.5	4.18
	b	0.95	0.02	0.02	0.01	0.95	0.5	0.18	0.43	0.66	99.82	0.49	4.26
May	a	0.95	0.03	0.03		0.94	0.53	0.19	0.47	0.69	99.81	0.43	4.73
	b	0.95	0.02	0.02	0.01	0.94	0.52	0.18	0.46	0.68	99.82	0.42	4.84
Jun	a	0.95	0.02	0.03		0.94	0.55	0.19	0.53	0.72	99.81	0.3	6.59
	b	0.95	0.02	0.02	0.01	0.95	0.53	0.18	0.49	0.7	99.82	0.29	6.67
Jul	a	0.94	0.03	0.03		0.93	0.61	0.21	0.64	0.8	99.79	0.32	6.52
	b	0.94	0.02	0.02	0.02	0.94	0.6	0.2	0.61	0.78	99.8	0.3	6.66
Aug	a	0.93	0.03	0.03		0.93	0.62	0.21	0.64	0.8	99.79	0.37	5.59
	b	0.93	0.02	0.03	0.02	0.93	0.6	0.21	0.62	0.79	99.79	0.36	5.67
Sep	a	0.94	0.03	0.03		0.93	0.58	0.2	0.56	0.75	99.8	0.37	5.34
	b	0.94	0.02	0.02	0.02	0.94	0.56	0.2	0.53	0.73	99.8	0.38	5.3
Oct	a	0.94	0.03	0.03		0.94	0.53	0.19	0.47	0.68	99.81	0.4	4.86
	b	0.94	0.02	0.03	0.02	0.94	0.53	0.19	0.46	0.68	99.81	0.4	4.81
Nov	a	0.95	0.02	0.03		0.95	0.55	0.2	0.52	0.72	99.8	0.39	6
	b	0.95	0.01	0.02	0.01	0.95	0.54	0.2	0.51	0.72	99.8	0.4	5.88
Dec	a	0.96	0.02	0.02		0.96	0.55	0.2	0.54	0.73	99.8	0.34	9.12
	b	0.96	0.01	0.01	0.01	0.96	0.57	0.21	0.56	0.75	99.79	0.36	8.93

Model a: [sta_mean ~ "ptmean", "hli", "dem"]
Model b: [sta_mean ~ "ptmean", "hli", "dem", "vrm"]

S6. Available water capacity

The Newhall simulation model used to simulate water movement relied on a single available water capacity (AWC) value for the soil profile (defined as a 30 m pixel), which relates to the soil properties at a given cell. Here, we explain how we calculated AWC. Field capacity is the water remaining in the soil after thoroughly saturated and allowed to drain freely, usually for one to two days, and has a tension of ~33 kPa. Permanent wilting point is the moisture content of a soil where plants wilt and fail to recover when supplied with sufficient moisture. The permanent wilting point depends on plant variety, and most plants require ~1,500 kPa of tension to extract water from the soil. Water capacity is usually expressed as a volume fraction, percentage, or depth (in or cm). We estimated the field capacity and wiling point (*theta*) using the Van Genuchten method [eq. 1; 51]. The $theta_r$ (wilting point as m^3m^{-3}) and $theta_s$ (field capacity as m^3m^{-3}) Polaris data are estimated with the pedotransfer function NeuroTheta, which relates observed soil properties to hydraulic properties [6]. At a given *pressure* (-33 kPa for field capacity and -1,500 kPa for wilting point), we calculated $theta_h$ (soil water content, where *h* reflects the saturated [-33 kPa] or residual [-1,500 kPa] conditions) at 6 soil depths (0 – 5 cm, 5 – 15 cm, 15 – 30 cm, 30 – 60 cm, 100 – 200 cm) using the median estimate of each Polaris data property of each parameter ($theta_s$, $theta_r$, *n*, and *m*) and the Van Genuchten method (eq. 1). For each soil depth represented in the Polaris data, we calculated AWC_i (eq. 2) based on the estimated saturated and residual soil water content calculated (eq. 1).

$$theta_h = theta_r + \frac{(theta_s - theta_r)}{(1 + abs(alpha * pressure)^n)^m}, \quad (1)$$

where $theta_s$ is the saturated soil water content (m^3/m^3), $theta_r$ is the residual soil water content (m^3/m^3), *alpha* is the scale parameter inversely proportional to mean pore diameter (van Genuchten; log10(kPa-1)), *n* is the measure of the pore size distribution (van Genuchten; unitless), and *m* is 1 - (1/*n*). $theta_h$ is either $theta_{33}$, soil water content at field capacity (m^3/m^3) or $theta_{1500}$, soil water content at the wilting point (m^3/m^3).

$$AWC_i = theta_{s,i} - theta_{r,i} \quad (2)$$

where $theta_{s,i}$ is the saturated soil water content and depth *i*, and $theta_{r,i}$ is residual soil water content at depth *i*.

While calculating $theta_h$ for depth 5 – 15 cm, we discovered an issue with the Polaris data where the results had values of zero for most pixels. Because we could not correct $theta_h$, we averaged AWC_i depths of 0 – 5 cm and 15 – 30 cm based on how AWC changed across the remaining soil depths. We also populated no data values within the derived AWC_i, inherited from the Polaris data, using valid values from nearest neighbor pixels (section S1). We calculated a single AWC for the soil profile (each pixel) by summing the midpoint of the AWC associated with each depth range [eq. 3; 52].

$$AWC = \sum (awc_i * thickness), \quad (3)$$

where awc_i is AWC (as m^3m^{-3}) for a given depth range (0 – 5 cm, 5 – 15 cm, 15 – 30 cm, 30 – 60 cm, 100 – 200 cm) and *thickness* is the soil thickness associated with each range, respectively 5 cm, 10 cm, 15 cm, 30 cm, and 100 cm. The multiplication thickness and awc_i converted the volumetric units to cm, as required by the Newhall model.

S7. Potential evapotranspiration

Potential evapotranspiration (PET) describes the amount of evaporation and transpiration (combined water loss) that is expected (calculated) to occur when sufficient water is available within the soil [53]. Due to the ambiguity of the PET definition, most studies estimate reference ET (ET_0) using several additionally defined variables, such as assuming a hypothetical reference crop with a height of 0.12-m and fixed surface resistance and albedo [e.g., 54,55]. The PET can be measured using lysimeter instruments but is more frequently estimated using theoretical or empirical equations [e.g., 56,57]. Of the more than 50 approaches to estimating ET_0 [58], there are temperature-based, radiation-based, and combination-based approaches [e.g., 57,59]. Many studies have compared the different models with varying results due to differences in equations, data inputs, scale, climate conditions, and application [e.g., 55,56,59-63].

Some of the more commonly used temperature-based methods include Thornthwaite-Mather-Sellers [53,64,65], Hargreaves-Samani [66], and Hamon [62,67]. Commonly used radiation-based methods include various forms of Penman-Monteith [68], Priestley-Taylor [69], and Makkink [70]. Recent research suggests using energy-based equations for finer temporal scales, recognizing these are only more precise if accurate data exist for estimating parameters and the geographic region does not have sizeable monthly temperature ranges [71]. Food and Agriculture Organization (FAO) of the United Nations identified the Penman-Monteith equation (FAO-56 PM) as the standard method for estimating reference evapotranspiration (ET_0) and Hargreaves as an alternative when climate data is unavailable for FAO-56 PM methods [e.g., wind; 54].

Thornthwaite and Mather [64,72] found that potential evapotranspiration was a function of average air temperature, latitude, and length of day, where estimates are based upon a 12-hour day (amount of daylight) and a 30-day month (equations shown below). Tables of PET referenced in Thornthwaite and Mather [64] were criticized for estimating low values in winter and high in the summer [73]. However, Thornthwaite and Mather [72] had used non-linear relationships via log-log graphs and therefore were not estimating low winter or high summer PET values [73]. Additionally, the original Thornthwaite and Thornthwaite-Mather equations were intended to describe PET between 0°C and 26.5°C, where evapotranspiration exponentially increases with temperature. Sellers [65] modifies the equations to account for PET between 26.5°C and 38°C, where the relationship between temperature and PET follows a parabolic function. Research also suggests that Thornthwaite's equation accurately accounts for monthly PET and is accepted for such applications, but because it was developed with data from humid climates, its performance generally underestimates PET in semi-arid climates [59,74].

In summary, Thornthwaite [53] used different models for hot and cool months while also specifying a limit of 26.5°C. Below 26.5°C, the same monthly mean temperature generated lower PET in hot climates than cool climates, which is accounted for with a heat index [64,72]. Sellers [65] provided equations for PET between 26.5°C and 38°C. The varying forms of Thornthwaite equations do not correct for different vegetation types, cloud cover, and snow cover, but no PET models account for these factors. Due to the persistent use of Thornthwaite in the United States and our need to assess monthly climate normals and climate projections, we

used Thornthwaite-Mather-Sellers [53,64,65]. The Newhall simulation model (software) references tables from Thornthwaite [53], but we have provided equations below reflecting the computation methods reflected in the software. Our software (*nsm_spatial*) will also support substituting different PET equations for other applications.

The Thornthwaite-Mather equation with Sellers (1965) modification for $26.5°C < T_i \leq 38.0°C$:

If $T_i < 0°C$

$$mpe = 0$$

If $T_i < 32°F$

$$mpe = 0$$

If Celsius: $0°C < T_i < 26.5°C$

$$mpe = lcf * 16\left(10\ x\ \frac{T_i}{I}\right)^a$$

If Fahrenheit: $32°F < T_i < 79.4°F$

$$mpe = lcf * 0.63\left(50\left(\frac{(T_i - 32)}{9I}\right)\right)^a$$

where *lcf* is the latitude correction factor, T_i is monthly mean temperature, and *I* is the annual heat index. This index is used in the southern hemisphere only.

1. Monthly heat index (*i*) as a function of the average monthly temperature

   Celsius: $i = mwi = \left(\frac{T_i}{5}\right)^{1.514}$

   Fahrenheit: $i = mwi = \left(\frac{(T_i - 32)}{9}\right)^{1.514}$

2. Annual heat index (*I*)

   $$I = swi = \sum_{1}^{12} i$$

3. Alpha-constant based on annual heat index

   $a = (6.75x10^{-7}I^3) - (7.71x10^{-5}I^2) + (1.792x10^{-2}I) + 4.9239x10^{-1}$

4. Latitude correction factor

   The latitude correction factor is based on the number of daylight hours per month, which is a function of solar declination and latitude.

   lcf = (daylight hours for entire month)/(12 * number of days in month)
   Daylight hours per day = (24/π) * (ArcCos(-Tan(latitude) * (Tan(solar declination)))
   Latitude (radians) = (2π * latitude (degrees))/360
   Solar declination (radians) = 0.4093 * Sin(((2πJ)/365) – 1.405)

J = Julian day number

If $26.5°C < T_i \leq 38.0°C$

$$mpe = -41.947 + 3.246(T_i) - 0.0436(T_i)^2$$

If $79.7°F < T_i < 100.4°F$

Unknown

If $T_i \geq 38°C$

$$mpe = 185.0$$

If $T_i \geq 100.4°F$

$$mpe = 185.0$$

S8. Newhall simulation overview

The Newhall soil simulation model was documented by a progression of publications that describe its functions and application [75-78] especially the methods used to simulate soil water accretion and depletion and classify soil temperature and moisture regimes. The Newhall model operates on a soil moisture profile with eight vertical layers, where the second and third layers of the soil profile comprise the soil moisture control section (SMCS). The model uses the SMCS to define the soil moisture and temperature regimes at an average 50 cm soil depth (sections S9 and S10). The upper SMCS boundary represents a depth where dry soil can be moistened with 25 mm of water within 24 hours. The lower region of the SMCS boundary occurs at a depth where dry soil can be moistened with 75 mm of water within 48 hours. Dry soils have a water tension of >1500 kPa, meaning the water is unavailable to most mesophyte plants (i.e., plants not explicitly adapted to dry or wet environments). The Newhall model divides each layer of the soil profile into eight cells, forming a matrix of eight rows by eight columns, where each cell will represent $1/64^{th}$ of the total available water capacity (AWC) associated with the soil profile.

Vertical water movement within a soil profile is simulated in an 8-by-8 matrix while accounting for water accretion (added) and depletion (removed) occurring daily within a month (assumed as 30-days). This simulated movement expresses the monthly net balance of soil moisture based on a daily simulation [76,77]. The process of water infiltrating and evaporating from the soil is affected by evapotranspiration and the AWC associated with the soil properties, such as rock fragments, organic matter, bulk density, osmotic pressure, soil texture, and rooting depth [79]. Water is added (accretion) to the profile from top to bottom (layers) and left to right (slots/cells). Removal of water (depletion) from the soil occurs via PET (energy) by starting with the top right-hand slot and moving left and then diagonally downward. The depletion rate is inversely proportional to the tension holding the water and the depth of the layer. The process of accretion and depletion is also partially described in Van Wambeke [76].

The Newhall simulation of water accretion and depletion approximates the intensity and amount of precipitation input based on two types of rain events applied at the first 15-days, mid-month, and last 15-days of each month. Light precipitation (LP = monthly precipitation/2) is applied at the beginning and end of the month, where accretion and depletion can occur, and heavy precipitation (HP = monthly precipitation/2) is applied mid-month when only accretion

occurs. Net potential evapotranspiration (NPE) is used to assess whether accretion (NPE > 0 in slot) or depletion (all LP expended, soil profile reaches AWC, or NPE ≤ 0) occurs, which is calculated during the first and last 15 days of each month [NPE = (LP – MPE)/2]. During accretion, the AWC is reduced by NPE, and during depletion, a depletion rate is applied based on the location of the cell as defined in the simulation [76,77]. The Newhall simulation model first establishes a stable soil moisture conditioning period within the soil profile by enumerating the monthly simulation until the moisture on Dec. 30th is <1/100 of the moisture on Dec. 30th of the preceding iteration.

During the last simulation run of the conditioning period, the model tracks the moisture state (dry in all parts, dry and moist in some parts, and moist in all parts) and its duration during each month's first and last rain event stage. Specifically, it tracks the moisture condition classification for each day and summarizes the number of days and cumulative days associated with each moisture condition classification: dry (D), both moist and dry (B), and moist (M). The moisture condition [dry, partial, wet] in the moisture control section is determined based on conditions recorded at three slots (9, 17, 25). Slot 25 falls outside the moisture control section, and therefore, it is used to determine the moisture condition signaling accretion or depletion. If all slots (9, 17, 25) are dry, then soil moisture condition is classified as dry (D). If slots include moist and dry conditions, then soil moisture condition is classified as some parts moist (B). If all slots are moist, soil moisture condition is classified as moist (M). The relative duration of the moisture condition is determined every two weeks, which is then used to update the cumulative number of days within the moisture control section. The relative duration is defined for each moisture condition, where the initial (I) soil moisture state captures the first rain event, and the final (F) soil moisture state captures the third rain event [heavy; 76,77]. If PET at a given time (NPE) is less than 0 and soil moisture condition changes from M to B or D during a half-month period, each condition's duration (days) is calculated using the following methods:

1) If I is moist (M) and F is both moist and dry (B), the duration of days for M = 15 * (NPE of transition I to B)/(NPE available) and duration of B = 15 – duration of days;
2) If I is moist and F is dry, the duration of days for M = 15 * (NPE of transition I to B)/(NPE available), the duration of days for B = 15 * (NPE of transition B to D)/(NPE available), and the duration of days for D = 15 – (duration of M + duration of B).

After the Newhall model defines the number of days occurring under dry, moist and dry, and moist soil conditions within the soil moisture control section, the model assesses the cumulative days and consecutive days (duration of the moisture condition) under different temperatures and seasons to inform the soil moisture regime classification.

Soil temperatures ≥5°C are considered biologically active because the respiration of micro-organisms can occur; however, in colder climates, biological activity may occur when soil temperatures fall below 5°C [80]. The thresholds of 5°C and 8°C are used in the Newhall simulation to track moisture conditions (dry, moist and dry, and moist) within the soil moisture control section, which are established for biological activity and major crops grown in the contiguous United States. The definitions of soil temperature and moisture regimes have changed little over time and are primarily based on biological activity, crop types, and soil groups [81-85]. For example, at 8°C ambient temperature, wheat (*Triticum aestivum* L.) is distinguished from corn (*Zea mays* L.) and identifies several soil groups in the northern United States [82].

Cotton (*Gossypium hirsutum* L.), pineapple (*Ananas comosus* [L.] Merr.), and sugarcane (*Saccharum officinarum* L.) grow at ≥15°C ambient temperature and identify several Great Soil groups in the southern United States [82].

The Newhall model tracks the soil moisture states and soil temperature to inform the classification of the soil moisture regime lastly. The following information is used for these classifications:

1) the number of consecutive seasonal (summer and winter) days under moist and dry conditions;
2) cumulative days where soil temperature above 5°C;
3) number of days where soil temperature <5°C;
4) the number of cumulative days in D, B, and M states;
5) the number of consecutive days in a B state;
6) the number of consecutive days in B state >8°C;
7) number of days dry after summer solstice;
8) number of days moist days after winter solstice;
9) daily temperature calendar where soil temperature <5°C;
10) soil temperature between 5°C and 8°C;
11) and >8°C.

The start and end days when the soil temperature is above or below a given critical value are approximated from the sequence of mean monthly temperatures. A summer lag phase (warming) is used to offset days when temperature <5°C. When soil temperature rises above a critical temperature, 21 days is added to the 15th day (equals 36 days) to compensate for the time lag between air and soil temperature at 50 cm. A winter lag phase (cooling) is used to offset days when temperature <5°C. When soil temperature falls below a critical temperature, ten days is added to the 15th day (equals 25 days) to compensate for the time lag between air and soil temperature at 50 cm. These lags improve the estimates of soil temperature and better reflect the effects of heat capacity due to seasonal changes.

Two different occurrences of temperature offsets exist as defaults within the Newhall simulation model, which are used to account for differences between air temperature and soil temperature at a 50 cm soil depth and seasonal lags. First, it uses a soil-air temperature offset based on mean annual air and soil temperature relationships [42,46,75]. The default soil temperature offset used in the model estimates that the soil is 2.5°C higher than the air temperature during, which is considered appropriate for the continental United States [42,46,75]. This soil-air temperature offset is used to adjust the annual temperature and average summer and winter temperatures. The offset is not used to adjust monthly temperatures or occurrences where snow could affect temperatures, and it only informs the classification of soil temperature and moisture regimes. Second, a soil-air relationship amplitude default is used to adjust the seasonal difference of average summer and winter temperature by a factor 0.66 (33% reduction in temperature) at 50 cm soil depth, which is considered appropriate for the continental United States [42,75]. This correction factor is only used when assessing differences between seasons and making determinations of the soil temperature and moisture classifications.

The soil moisture and temperature conditions are used for associating the soils with broad soil moisture and temperature regime classification (sections S9 and S10). The Newhall model

also defines a soil moisture budget (known as Thornthwaite moisture index [TMI] in mm) by cumulatively adding each month's precipitation within the season and removing PET (precipitation – PET). A negative value of TMI indicates the amount by which the precipitation fails to supply the potential water need of the soil, and a positive value of TMI suggests the amount of excess water available for soil moisture recharge and runoff [86]. Importantly, the TMI does not account for soil properties (e.g., AWC) and only precipitation and PET. Therefore, our software tracks the monthly soil moisture (SM), accounting for precipitation, PET, and AWC.

S9. Soil temperature classification

Soil moisture and temperature regimes identify site conditions when the mean annual precipitation is ±1 standard deviation (SD) of a 30-year normal [84]. Soil temperature regimes are based on mean annual soil temperatures at a depth of 50 cm (i.e., soil moisture control section) from the soil surface. These regimes greatly inform the use and management of soils, particularly for distribution of adapted plants. Iso soil temperature regimes distinguish between tropical and temperate soils where temperature differences are <6°C between summer (June, July, and August) and winter (December, January, and February). Instead of using pre-defined summer and winter months, we used the three coldest and three warmest months when assessing seasonal differences based on more recent research [83].

The Newhall model uses soil temperature at 50 cm and not ambient temperature, and therefore these thresholds will be several degrees cooler (summer) and warmer (winter) compared to ambient temperature. For consistency, we relied on the U.S. Department of Agriculture [USDA; 84,87] soil-climate classifications and the proposed temperature and moisture modifications of the International Soil Correlation Meeting [85]. The definitions of temperature regimes from the U.S. Department of Agriculture are mostly reflected within the jNSM 1.6.1 [88]. However, we used a key developed from the international workshop for consistency to address unclassified moisture regimes. Table S5 provides a list of acronyms used in the key.

Table S5. Variable names and definitions used within the software release (*nsm_spatial*) and referenced in the soil temperature classification key.

Variable corresponding to code	Definition
MAST	Mean annual soil temperature
MSST	Mean summer soil temperature
MWST	Mean winter soil temperature

U.S. Department of Agriculture temperature regime classification (Coldest to hottest)

1. pergelic
    - MAST <0°C at 50 cm below the surface. In this temperature regime, permafrost is present.
2. cryic

- MAST 0°C – 8°C, with no permafrost.
- The average summer temperature (with soil-air offset) minus the corrected seasonal difference (with seasonal amplitude) <15°C.
- Organic soils will have a MAST 0°C – 6°C.
- Mineral soils
    - If soil not saturated during some part of the summer and there is no *O* horizon, the mean summer temperature 0°C – 15°C
    - If soil not saturated during some part of the summer and there is an *O* horizon, the mean summer temperature 0°C – 8°C
    - If soil saturated during some part of the summer and there is no *O* horizon, the mean summer temperature 0°C – 13°C
    - If soil saturated during some part of the summer and there is an *O* horizon, the mean summer temperature 0°C – 6°C

3. frigid
    - MAST 0°C – 8°C, with a difference between mean summer and mean winter soil temperatures ≥6°C at 50 cm below the surface. The average summer temperature (with soil-air offset) minus the corrected seasonal difference (with seasonal amplitude) ≥15°C.
4. isofrigid
    - MAST 0°C – 8°C, with a difference between mean summer and mean winter soil temperatures <6°C at 50 cm. below the surface. The average summer temperature (with soil-air offset) minus the corrected seasonal difference (with seasonal amplitude) ≥15°C.
5. mesic
    - MAST 8°C – 15°C, and the difference between mean summer and mean winter soil temperatures is ≥6°C at 50 cm below the surface.
6. isomesic
    - MAST 8°C – 15°C and the difference between mean summer and mean winter soil temperatures <6°C at 50 cm below the surface.
7. thermic
    - MAST 15°C – 22°C; and a difference between mean summer and mean winter soil temperatures of ≥6 °C at 50 cm below the surface.
8. isothermic
    - MAST 15°C – 22°C and the difference between mean summer and mean winter soil temperatures <6°C at 50 cm below the surface.
9. hyperthermic
    - MAST ≥22°C and a difference between mean summer and mean winter soil temperatures ≥6°C at 50 cm below the surface.
10. isohyperthermic
    - MAST ≥22°C and the difference between mean summer and mean winter soil temperatures <6°C at 50 cm below the surface.
11. megathermic

- The MAST is ≥28°C and the difference between mean summer and mean winter soil temperatures of ≥6°C at 50 cm below the surface.

12. isomegathermic soil temperature regime
    - The MAST is ≥28°C and the difference between mean summer and mean winter soil temperatures <6°C at 50 cm below the surface.

International soil correlation meeting key (classification) of temperature regimes

We updated the soil temperature key developed during the International Soil Correlation Meeting [85], which had defined the difference between summer and winter soil temperature as 5°C, to reflect a 6°C difference of summer and winter soil temperature to reflect current views [84].

I. MAST ≥ 22°C
   A. MSST – MWST < 6°C [Isohyperthermic]
   B. MSST – MWST ≥ 6°C [Hyperthermic]

II. 15°C ≤ MAST < 22°C
   A. MSST – MWST < 6°C [Isothermic]
   B. MSST – MWST ≥ 6°C [Thermic]

III. 10°C ≤ MAST < 15°C
   A. MSST – MWST < 6°C [Isomesic]
   B. MSST – MWST ≥ 6°C [Mesic]

IV. 8°C ≤ MAST < 10°C
   A. MSST – MWST < 6°C [Isofrigid]
   B. MSST – MWST ≥ 6°C [Mesic]

V. MAST < 8°C
   A. MSST ≥ 15°C [Frigid]
   B. 13°C ≤ MSST < 15°C
      1. Soil not saturated with water during some part of summer and has no organic horizon [Cryic]
      2. Soil saturated with water during some part of summer or has an organic horizon [Frigid]
   C. 8°C ≤ MSST < 13°C
      1. MSST – MWST < 6°C [Isofrigid]
      2. MSST – MWST ≥ 6°C
         a. No organic horizon [Cryic]
         b. Has organic horizon [Frigid]
   D. 6 °C ≤ MSST < 8 °C
      1. MSST – MWST < 6°C [Isofrigid]
      2. MSST – MWST ≥ 6°C
         a. No organic horizon [Cryic]
         b. Has organic horizon
            1) Soil not saturated with water during some part of summer [Cryic]

2) Soil saturated with water during some part of summer [Frigid]

E. MSST < 6°C
   1. MAST > 0°C
      a. MSST – MWST < 6°C [Isofrigid]
      b. MSST – MWST ≥ 6°C [Cryic]
   2. MAST ≤ 0°C
      a. MSST – MWST < 6°C [Isofrigid]
      b. MSST – MWST ≥ 6°C [Pergelic]

S10. Soil moisture classification

Soil moisture and temperature regimes reflect a year when the mean annual precipitation is ±1 SD of 30-year normal [84]. Soil moisture regimes characterize the conditions of groundwater or water held at a tension of 1,500 kPa in the soil, where a tension >1,500 kPa is considered dry because most plants cannot access the water, and a tension <1,500 kPa is considered wet [84].

The aquic soil moisture regime is not represented here because these soil types are typically challenging to classify programmatically, and suitable data to accurately represent those soil conditions across broad landscapes is not available. Based on the USDA soil handbook [84], the aquic moisture regime does not have dissolved oxygen because the soil is saturated with water. The duration of an aquic soil to be saturated is not defined by USDA, but this should be at least a few days. Aquic soils will have soil temperature above biologic zero (5°C in this taxonomy, but this can be lower in very cold environments) for some duration because dissolved oxygen is removed from groundwater by respiration of micro-organisms, roots, and soil fauna. Soils with groundwater very close to the surface, such as tidal marshes or landlocked depressions fed by perennial streams, are classified as a peraquic moisture regime. Historically aquic soils have been mapped and not classified using any model [41].

We updated the soil moisture key developed during the International Soil Correlation Meeting [85], which had defined the difference between summer and winter soil temperature as 5°C, to reflect a 6°C difference of summer and winter soil temperature to reflect current views [84]. We also added definitions for Perudic soil moisture regime and soil moisture regime subdivisions based on USDA [84]. Table S6 provides a list of abbreviations/acronyms used in the key.

Table S6. Variable names and definitions used within the software release (nsm_spatial) and included in the soil moisture classification key.

Variable corresponding to code	Definition
dif	Seasonal difference of average summer and winter temperature
fcd	Corrected seasonal amplitude when calculating seasonal temperatures
MAST	Mean annual soil temperature
MSST	Mean summer soil temperature
MWST	Mean winter soil temperature

Variable corresponding to code	Definition
nccd	Days dry after summer solstice
nccm	Moist days after winter solstice
ncpm[1]	Number of consecutive days moist in some places of the moisture control section
ncpm[2]	Number of consecutive dry and moist days over 8°C in some places
nd[1]	Number cumulative days dry
nd[2]	Number cumulative days moist and dry
nd[3]	Number cumulative days moist
nsd[1]	Cumulative days dry over 5°C
nsd[2]	Cumulative days moist and dry over 5°C
nsd[3]	Cumulative days moist over 5°C
SMCS	Soil moisture control section
tma	Annual temperature with an applied soil-air temperature offset
trr	Temperature regime classification

U.S. Department of Agriculture temperature regime classification (wettest to driest)

1. Aquic (or Perudic): These very moist soils occur in tidal marches, landlocked depressions with perennial streams, and similar circumstances where the soils are saturated with water long enough to cause oxygen depletion.
   A) Precipitation (PPT) exceeds ET in all months.
   B) This is not applicable to soils with <5°C during saturation (days or longer).
   C) This regime is not defined on an annual basis and therefore aquic soils can also be classified as xeric, ustic, or aridic.
   D) These generally pertain to mineral soils and have reduced iron. Aquic conditions were later introduced because Aquic soil moisture regime (SMR) not consistently applied across United States or clearly defined [89], which is why they recommended dropping Aquic SMR.
2. Udic: Humid or subhumid climate. The amount of stored moisture is approximately equal to the amount of evapotranspiration.
   A) The SMCS is not dry in any part for ≥90 cumulative days in a normal year (i.e., moist in all parts for ≥90 cumulative days in a year)
   B) If MAST <22°C and mean winter and mean summer soil temperature difference at 50 cm by ≥6°C, the SMCS is dry in all parts for <45 consecutive days in the summer.
   C) Requires a three-phase system (soil-liquid-gas) in SMCS when soil temperature >5°C.
   D) Have at least nine months when the SMCS is completely moist. However, at least one month has some dryness; some soils dry out completely in the control section but seldom for more than one month.

- Typic Udic: dry in some or all parts <30 cumulative days.
- No existence of isotemperature regime: (dif * fcd) ≥6℃:
    - Dry Tempudic: Dry in some or all parts ≥30 cumulative days.
- Existence of isotemperature regime: (dif * fcd) <6℃
    - Dry Tropudic: Dry in some or all parts ≥30 cumulative days.

3. Ustic: Semiarid climate (intermittently moist and dry where moisture exists when conditions suitable for plant growth). Regions with a ustic soil moisture regime often experience erratic rainfall, mainly occurring during the growing season. Summer droughts are erratic but frequent. This is not applied to soils that have permafrost (pergelic) or cryic soil temperature regimes.
    A) If the MAST is ≥22℃ OR the mean summer and winter soil temperatures differ by <6℃ (iso-temperature), the SMCS is dry in some or all parts for ≥90 cumulative days, but moist in some part for >180 cumulative days per year OR for moist in some part for ≥90 consecutive days.
    B) If the MAST <22℃ AND the mean summer and winter soil temperatures differ by ≥6℃, the SMCS is dry in some or all parts for ≥90 cumulative days, but it is not dry in all parts for more than half of the cumulative days when the soil temperature is >5℃.
    C) If the SMCS moist in all parts for ≥45 consecutive days in the 4 months following the winter solstice, the SMCS is dry in all parts for <45 consecutive days in the 4 months following the summer solstice. Summer solstice (June 20) and winter solstice (Dec 21)
    D) In tropical/subtropical regions with monsoons and one or two dry seasons (summer and winter seasons differ little), there is a least one rainy season for ≥3 or more months.

    - No existence of isotemperature regime:
        - Wet Tempustic: Moist in all parts ≥45 consecutive days in winter and not dry ≥45 consecutive days in summer
        - Typic Tempustic: Dry in some or all parts ≥90 cumulative days in winter; not dry in all parts >half cumulative days when soil temp >5℃
        - Xeric Tempustic: Meets moisture criteria for the Xeric SMR but has a MAST ≥22℃.
    - Existence of isotemperature regime:
        - Aridic Tropustic: partly or completely moist for <180 consecutive days
        - Typic Tropustic: partly or completely moist for ≥180 and <270 consecutive days
        - Udic Tropustic: partly or completely moist for ≥270 consecutive days

4. Xeric: Mediterranean-type climate, which has moist, cool winters and dry, warm summers.
    A) SMCS dry in all parts for ≥45 consecutive days in 4 months following summer solstice AND moist in all parts ≥45 consecutive days in 4 months following winter solstice,

B) AND SMCS is moist in some part for more than half of the cumulative days per year when the soil temperature is >5℃ OR for ≥90 consecutive days when the soil temperature is >8℃,
C) AND the MAST <22℃,
D) AND the mean summer and mean winter soil temperatures differ by ≥6℃.

- Typic Xeric: Dry in all parts 45 to ≤90 consecutive days in summer
- Dry Xeric: Dry in all parts >90 consecutive days in summer

5. Aridic (or Torric): Arid climate.
   A) Dry in all parts for more than half of the cumulative days per year when the soil temperature is >5℃,
   B) AND moist in some or all parts for <90 consecutive days when the soil temperature is >8℃.

- Weak Aridic: Moist in some or all parts >45 but <90 consecutive days when soil temp >8℃
- Typic Aridic: Moist in some or all parts ≤45 consecutive days when soil temp >8℃
- Extreme Aridic: Completely dry during the entire year

International soil correlation meeting key (classification) of soil moisture regimes

We updated the soil temperature key developed during the International Soil Correlation Meeting [85], which had defined the difference between summer and winter soil temperature as 5°C, to reflect a 6°C difference of summer and winter soil temperature to reflect current views [84].

I. PPT > PET per month for all months and during saturation daily temperature ≥ 6°C [Perudic]
II. Moist in all parts for > t_{275} cumulative days most years (not dry in any parts ≥ t_{90}) (nd[3] > 275 and not (nd[1] + nd[2] ≥ 90))
    A. MAST ≥ 22°C [Udic] (tma ≥ 22)
    B. MAST < 22°C (tma < 22)
        1. MSST – MWST < 6°C [Udic] (dif < 6°C)
        2. MSST – MWST ≥ 6°C (dif ≥ 6°C)
            a. Dry in all parts ≥ t_{45} consecutive days in the 4 months after the summer solstice in normal years [Xeric] (nccd ≥ 45)
            b. Not dry in all parts ≥ t_{45} consecutive days in the 4 months after the summer solstice in normal years [Udic] (nccd < 45)
III. Dry in some or all parts for ≥ t_{90} cumulative days most years (nd[3] <= 275 and nd[1] + nd[2] > 90).
    A. Cryic or Pergelic soil temperature classification (trr in [“Cryic”, “Pergelic”])
        1. MSST – MWST < 6°C [Aridic] (dif < 6°C)

2. MSST – MWST ≥ 6°C (dif ≥ 6°C)
    a. Dry in all parts for ≥ t_{45} consecutive days in the 4 months after the summer solstice in normal years and moist in all parts ≥ t_{45} consecutive days in the 4 months after the winter solstice in normal years [Xeric] (nccd ≥ 45 and nccm ≥ 45)
    b. Not both dry in all parts for ≥ t_{45} consecutive days in the 4 months after the summer solstice in normal years and moist in all parts ≥ t_{45} consecutive days in the 4 months after the winter solstice in normal years [Aridic] (nccd >= 45) or (ncpm[1] >= 45) or (nccm >= 45)

B. Not Cryic and not Pergelic soil temperature classification (trr not in ["Cryic", "Pergelic"])
    1. MAST ≥ 22°C (tma ≥ 22)
        a. Moist in some parts for > t_{180} cumulative days [Ustic] (nd[2] > 180) or (ncpm[1] ≥ 90)
        b. Not moist in any parts for > t_{180} cumulative days (nd[1] > 180)
            1) Moist in some or all parts for ≥ t_{90} consecutive days [Ustic] (ncpm[1] + ncpm[2] ≥ 90)
            2) Not moist in any parts for ≥ t_{90} consecutive days [Aridic] (ncpm[1] ≤ 90)
    2. MAST < 22 °C (tma < 22)
        a. MSST – MWST < 6°C (dif < 6°C)
            1) Moist in some or all parts for > t_{180} cumulative days [Ustic] (nd[2] + nd[3] > 180)
            2) Not moist in any part for > t_{180} cumulative days (nd[1] > 180)
                a) Moist in some or all parts for ≥ t_{90} consecutive days [Ustic] (ncpm[1] ≥ 90)
                b) Not moist in any part for ≥ t_{90} consecutive days [Aridic] (ncpm[1] < 90)
        b. MSST – MWST ≥ 6°C (dif ≥ 6)
            1) Moist in some or all parts for $t_{1/2}$ cumulative days when soil temperature > 5°C (nsd[2] + nsd[3] > ((nsd[1] + nsd[2] + nsd[3])/2))
                a) Dry in all parts for ≥ t_{45} consecutive days in the 4 months after the summer solstice in normal years and moist in all parts for ≥ t_{45} consecutive days in the 4 months after the winter solstice in normal years [Xeric] (nccd ≥ 45 and nccm ≥ 45)
                b) Not both dry in all parts for ≥ t_{45} consecutive days in the 4 months after the summer solstice in normal years and moist in all parts for ≥ t_{45}

consecutive days in the 4 months after the winter solstice in normal years [Ustic] (nccd ≥ 45) or (nccm ≥ 45)

c) [NEW] Dry in some part for ≥ 90 cumulative days, but dry in all parts for <45 consecutive days in summer [Ustic] (nd[2] ≥ 90) and (nccd < 45)

2) Dry in all parts for ≥ $t_{1/2}$ cumulative days when soil temperature > 5°C (nsd[1] ≥ ((nsd[1] + nsd[2] + nsd[3])/2))

a) Moist in some or all parts ≥ t_{90} consecutive days where soil temperature > 8°C (ncpm[2] ≥ 90)

1) Dry in all parts for ≥ t_{45} consecutive days in the 4 months after the summer solstice in normal years and moist in all parts for ≥ t_{45} consecutive days in the 4 months after the winter solstice in normal years [Xeric] (nccd ≥ 45 and nccm ≥ 45)

2) Not both dry in all parts for ≥ t_{45} consecutive days in the 4 months after the summer solstice in normal years and moist all parts for ≥ t_{45} consecutive days in the 4 months after the winter solstice in normal years [Ustic] (nccd ≥ 45) or (nccm ≥ 45)

3) [NEW] Dry in some part for ≥ 90 cumulative days, but dry in all parts for <45 consecutive days in summer [Ustic] (nd[2] ≥ 90) and (nccd < 45)

b) Not moist in any parts for ≥ t_{90} consecutive days when soil temperature ≥ 8°C [Aridic] (ncpm[2] < 90)

Soil moisture subdivisions

Although soil moisture subdivisions [75] are used in various studies [9,40,90] and within the *jNSM* 1.6.1 software [88], they are not official or defined in the current USDA handbook [84]. The classifications are intended for classifying the landscape into soil-climate bins, and the subdivisions are interpreted as *soil moisture class bordering on soil moisture subclass*. We have added additional subdivisions for greater granularity within some soil moisture regimes (i.e., Perudic, Udic, Ustic, Xeric, and Aridic)—denoted as "New" below. The moisture subdivisions below reflect those defined in *jNSM* 1.6.1, unless noted as [New].

1. Perudic

- None None

2. Udic
    - [New] Wet Udic (nd[1] + nd[2] < 20)
    - Typic Udic (nd[1] + nd[2] ≥ 20 and nd[1] + nd[2] < 45)
    - Dry Tempudic (dif ≥ 6 and nd[1] + nd[2] ≥ 45 and nd[1] + nd[2] < 65)
    - [New] Dryer Tempudic (dif ≥ 6 and nd[1] + nd[2] ≥ 65)
    - Dry Tropudic (dif < 6 and nd[1] + nd[2] ≥ 45 and nd[1] + nd[2] < 65)
    - [New] Dryer Tropudic (dif < 6 and nd[1] + nd[2] ≥ 65)
3. Ustic
    - Wet Tempustic (dif ≥ 6 and nccm ≥ 45 and nccd < 45)
    - Typic Tempustic (dif ≥ 6 and not Wet and not Xeric Tempustic)
    - Xeric Tempustic (dif ≥ 6 and nccd ≥ 45 and nccm ≥ 45)
    - Aridic Tropustic (dif < 6 and ncpm[2] < 180)
    - Typic Tropustic (dif < 6 and ncpm[2] ≥ 180 and ncpm[2] < 270)
    - Udic Tropustic (dif < 6 and ncpm[2] ≥ 270)
4. Xeric
    - [New] Weak Xeric (nccd ≥ 45 and nccd < 65)
    - Typic Xeric (nccd ≥ 65 and nccd < 90)
    - Dry Xeric (nccd ≥ 90)
5. Aridic
    - Weak Aridic (ncpm[1] ≥ 45 and ncpm[2] < 180)
    - Typic Aridic (ncpm[2] ≥ 22 and ncpm[2] < 45)
    - [New] Dry Aridic (ncpm[2] ≥ 15 and ncpm[2] < 22)
    - Extreme Aridic (ncpm[2] < 15 or (nd[1] + nd[2] ≥ 350))

S11. Comparative evaluation of Newhall simulation model software

nsm_spatial versus jNSM (v. 1.6.1): To ensure a direct comparison when evaluating results produced from *nsm_spatial* and *jNSM*, we removed most enhancements in *nsm_spatial* (see *section 2.7* and Table 2 in main manuscript). The *jNSM* software does not account for several factors that affect soil moisture and temperature, which we added or corrected within *nsm_spatial.* However, we could not easily change some modifications in *nsm_spatial* for a one-to-one comparison (e.g., use of soil temperature and moisture classification keys, inclusion of organic matter in classifying temperature, and attenuation of soil temperature and evaporation due to snow cover). Therefore, these differences remained, which will account for some of the differences in our comparative testing. The *jNSM* only works on Windows 7 operating systems, so we commandeered an old computer and tested off the network, as this operating system is no longer supported or allowed for use on government networks. The *jNSM* code relied on ten iterations where the NSM simulates moisture conditions until convergence occurs, which Newhall defined as when moisture on Dec. 30th becomes <1/100th of the moisture on Dec. 30th of the preceding iteration. We changed the number of iterations in *nsm_spatial* because the simulations were not always converging, and we evaluated both scenarios. Data inputs for both

tests included snowmelt adjusted precipitation, downscaled temperature, a default AWC of 200 mm, and a default air-soil temperature offset of 2.5°C for comparative testing. Results are reported in Table S7.

Table S7. Evaluation of 1,280 climate stations using identical input data and originating java Newhall simulation model software (*jNSM* 1.6.1) or our Python version (*spatial_nsm*) resulted in 48 occurrences where climate stations had different soil moisture regimes between *jNSM* and Python NSM. There were 24 climate stations where *jNSM* assigned Undefined soil moisture where *spatial_nsm* did not.

***jNSM* result**			***nsm_spatial* result**			
Moisture regime	**Moisture regime class**	**Moisture regime sub-class**	**Moisture regime**	**Moisture regime class**	**Moisture regime sub-class**	**Count**
Xeric	Typic	Xeric	Xeric	Dry	Xeric	7
Xeric	Typic	Xeric	Xeric	Typic	Xeric	1
Xeric	Typic	Xeric	Aridic	Weak	Aridic	1
Xeric	Dry	Xeric	Aridic	Weak	Aridic	2
Udic	Dry	Tempudic	Udic	Typic	Udic	7
Udic	Dry	Tempudic	Ustic	Wet	Tempustic	3
Ustic	Typic	Tempustic	Udic	Dry	Tempudic	2
Ustic	Typic	Tempustic	Ustic	Wet	Tempustic	5
Ustic	Typic	Tempustic	Aridic	Weak	Aridic	4
Aridic	Typic	Aridic	Aridic	Extreme	Aridic	8
Aridic	Typic	Aridic	Aridic	Weak	Aridic	8

S12. Description of data products

We describe the soil-climate spatial data products produced from our research (Table S8), information about a second mask where pixels coincide with features where there is likely an absence of soil (section S1; Polaris mask), and a Pearson R correlation matrix of soil-climate data products (Figure S5). We expected high correlation among soil moisture products as indicated in Figure S5 (patterns will be similar), but the distribution of the data (values) differs. Therefore, any one of the variables could be a better predictor if used in a model or for assessing trends and seasonality. Our soil moisture products reflect a measure of moisture remaining within the soil profile based on soil properties, potential evapotranspiration, monthly climate normal data (1981 – 2010) averaged over a 30 meter by 30-meter pixel. These values best describe relative moisture within soil across the landscape, which are well suited for understanding species' distributions, invasibility, wildfire potential, patterns/anomalies of soil moisture, and similar applications supporting rangeland and habitat management. The high correlation among soil moisture data products indicates similar patterns,

Units of continuous soil moisture: We calculated available water capacity (AWC) for a 30-m x 30-m pixel to a depth of 200 cm (2-m), which denotes the potential water capacity in mm for a given pixel. The precipitation model input was measured in millimeters. Therefore, the soil moisture content used in our products can be expressed as mm (similar to rainfall units), representing the amount of water remaining at the end of a month after evapotranspiration and

loss to runoff or atmosphere radiation forcing. We can also calculate the volume of water remaining in the soil (i.e., soil moisture per pixel) using dividing the soil moisture (mm) by 2,000 mm to obtain units of m^3m^{-3}).

Units of continuous Theil-Sen estimator: Theil-Sen is the median of slopes of all lines fitted with different combinations of paired points. Therefore, units represent mm/time, where time may be expressed in our case as March to June (4 months) or March to September (7 months). For example, if we have a value of 20 for Theil-Sen estimator of March to June, this is expressed as a median of 20 mm/month.

Units of seasonal variability: The annual, spring, summer, fall, and winter products were derived by calculating the average soil moisture (mm) for a specified period. Therefore, the units are mm and reflect average soil moisture.

Units of Seasonality: We calculated seasonality for two periods, including growing season (March, April, may, and June in Northern Hemisphere or September, October, November, and December in Southern Hemisphere) and seasonal (spring, summer, fall, and winter). The units for seasonality are expressed in mm and reflect the standard deviation of soil moisture.

Thornthwaite moisture index (TMI) versus soil moisture content: Both forms of these indices use units of mm. Unlike soil moisture, TMI does not account for potential available water capacity. The TMI is a simple measure of soil moisture, which the Newhall model originally defined for showing contours of soil moisture.

Table S8. Description of soil-climate data products produced from our implementation of the Newhall simulation modeling framework applied to the western United States between 1981 and 2010 (climate normal). Products include Thornthwaite moisture index (TMI) and soil moisture as (mm). 'Seasonal' products reflect seasonality (standard deviation) for spring, summer, fall, and winter. 'Trend' products reflect Theil-Sen estimate for March to June and March to September, providing the rate of change in soil moisture. All raster products based on a Conical Albers Equal Area with standard parallels appropriate for the contiguous United States and a 1984 World Geodetic System datum.

Filename	Description
annual_tmi_normal.tif	Summed monthly Thornthwaite moisture index (TMI; water balance) during year
spring_tmi_normal.tif	Summed monthly Thornthwaite moisture index (TMI; water balance) during spring (March to May)[1]
summer_tmi_normal.tif	Summed monthly Thornthwaite moisture index (TMI; water balance) during summer (June to August)
fall_tmi_normal.tif	Summed monthly Thornthwaite moisture index (TMI; water balance) during fall (September to November)
winter_tmi_normal.tif	Summed monthly Thornthwaite moisture index (TMI; water balance) during winter (December to February)
annual_sm_normal.tif	Summed monthly net soil moisture balance during year
spring_sm_normal.tif	Summed monthly net soil moisture balance during spring (March to May)

Filename	Description
summer_sm_normal.tif	Summed monthly net soil moisture balance during summer (June to August)
fall_sm_normal.tif	Summed monthly net soil moisture balance during fall (September to November)
winter_sm_normal.tif	Summed monthly net soil moisture balance during winter (December to February)
mar2jun_sm_normal_sd.tif	The standard deviation of monthly spring (March to June), net soil moisture balance (spring variability)
seasonal_sm_normal_sd.tif[1]	The standard deviation of seasonal (spring, summer, fall, and winter) net soil moisture balance
jan_sm_normal.tif	January net soil moisture balance
feb_sm_normal.tif	February net soil moisture balance
mar_sm_normal.tif	March net soil moisture balance
apr_sm_normal.tif	April net soil moisture balance
may_sm_normal.tif	May net soil moisture balance
jun_sm_normal.tif	June net soil moisture balance
jul_sm_normal.tif	July net soil moisture balance
aug_sm_normal.tif	August net soil moisture balance
sept_sm_normal.tif	September net soil moisture balance
oct_sm_normal.tif	October net soil moisture balance
nov_sm_normal.tif	November net soil moisture balance
dec_sm_normal.tif	December net soil moisture balance
trend_sm_mar2jun_normal.tif	Theil-Sen trend (median) estimate for early-growing (March to June) net soil moisture balance
trend_sm_mar2sep_normal.tif	Theil-Sen trend (median) estimate for growing period (March to September) net soil moisture balance
stmr_normal.tif	Soil moisture and temperature regime classification (discrete)
polaris_awc_mask.tif	Raster surface identifying where Polaris available water capacity (AWC) pixels had no data but were populated using AWC from nearest pixel.
nsm_mask.tif	Types of masked pixels that users may want to apply when working with soil-climate products. For example, available water capacity (AWC) estimates occurred where data were not relevant for terrestrial analyses of soil-climate (e.g., water body). These masks are broken into categories for aiding with masking and decision-making.

[1]Seasonal definitions: spring (March, April, and May), summer (June, July, and August), fall (September, October, and November), and winter (December, January, and February).

Figure S5. Pearson R correlation matrix of soil-climate data products produced from our implementation of the Newhall simulation modeling framework applied to the western United States from 1981 to 2010. The soil moisture (SM; units=mm) denotes the amount of water remaining in the soil profile after accounting for accretion and depletion of water simulated with the model and the soil properties described by available water capacity. Thornthwaite moisture index (TMI; units=mm) describes the net balance of precipitation input and potential energy affecting soil moisture (e.g., precipitation – PET). The SM and TMI were developed for each season (spring, summer, fall, and winter). Monthly data was defined for SM. Seasonality indices were defined as the standard deviation of all seasons (seasonality_std_sm, seasonality_std_tmi) and months occurring within a growing season (growing_std_spring_sm, growing_std_spring_tmi). Trend slopes were calculated using a Theil-Sen estimator for March to June (trend_mar2jun) and March to September (trend_mar2sep). Pearson R correlation was

calculated using 500,000 randomly distributed points with a minimum of 800 meters between points.

	jan_sm	feb_sm	mar_sm	apr_sm	may_sm	jun_sm	jul_sm	aug_sm	sep_sm	oct_sm	nov_sm	dec_sm	spring_sm	spring_tmi	summer_sm	summer_tmi	fall_sm	fall_tmi	winter_sm	winter_tmi	annual_sm	annual_tmi	growing_std_spring_sm	growing_std_spring_tmi	seasonality_std_sm	seasonality_std_tmi	trend_mar2jun	trend_mar2sep
jan_sm	1.0																											
feb_sm	1.0	1.0																										
mar_sm	1.0	1.0	1.0																									
apr_sm	1.0	1.0	1.0	1.0																								
may_sm	1.0	1.0	1.0	1.0	1.0																							
jun_sm	1.0	1.0	1.0	1.0	1.0	1.0																						
jul_sm	1.0	1.0	1.0	1.0	1.0	1.0	1.0																					
aug_sm	1.0	1.0	1.0	1.0	1.0	1.0	1.0	1.0																				
sep_sm	1.0	1.0	1.0	1.0	1.0	1.0	1.0	1.0	1.0																			
oct_sm	1.0	1.0	1.0	1.0	1.0	1.0	1.0	1.0	1.0	1.0																		
nov_sm	1.0	1.0	1.0	1.0	1.0	1.0	1.0	1.0	1.0	1.0	1.0																	
dec_sm	1.0	1.0	1.0	1.0	1.0	1.0	1.0	1.0	1.0	1.0	1.0	1.0																
spring_sm	1.0	1.0	1.0	1.0	1.0	1.0	1.0	1.0	1.0	1.0	1.0	1.0	1.0															
spring_tmi	1.0	1.0	1.0	1.0	1.0	1.0	1.0	1.0	1.0	1.0	1.0	1.0	1.0	1.0														
summer_sm	1.0	1.0	1.0	1.0	1.0	1.0	1.0	1.0	1.0	1.0	1.0	1.0	1.0	1.0	1.0													
summer_tmi	1.0	1.0	1.0	1.0	1.0	1.0	1.0	1.0	1.0	1.0	1.0	1.0	1.0	1.0	1.0	1.0												
fall_sm	1.0	1.0	1.0	1.0	1.0	1.0	1.0	1.0	1.0	1.0	1.0	1.0	1.0	1.0	1.0	1.0	1.0											
fall_tmi	1.0	1.0	1.0	1.0	1.0	1.0	1.0	1.0	1.0	1.0	1.0	1.0	1.0	1.0	1.0	1.0	1.0	1.0										
winter_sm	1.0	1.0	1.0	1.0	1.0	1.0	1.0	1.0	1.0	1.0	1.0	1.0	1.0	1.0	1.0	1.0	1.0	1.0	1.0									
winter_tmi	1.0	1.0	1.0	1.0	1.0	1.0	1.0	1.0	1.0	1.0	1.0	1.0	1.0	1.0	1.0	1.0	1.0	1.0	1.0	1.0								
annual_sm	1.0	1.0	1.0	1.0	1.0	1.0	1.0	1.0	1.0	1.0	1.0	1.0	1.0	1.0	1.0	1.0	1.0	1.0	1.0	1.0	1.0							
annual_tmi	1.0	1.0	1.0	1.0	1.0	1.0	1.0	1.0	1.0	1.0	1.0	1.0	1.0	1.0	1.0	1.0	1.0	1.0	1.0	1.0	1.0	1.0						
growing_std_spring_sm	-0.2	-0.2	-0.1	-0.1	-0.2	-0.3	-0.3	-0.4	-0.4	-0.4	-0.4	-0.3	-0.2	-0.5	-0.3	-0.6	-0.4	-0.4	-0.2	0.1	-0.3	-0.4	1.0					
growing_std_spring_tmi	0.7	0.7	0.7	0.7	0.7	0.7	0.7	0.7	0.7	0.7	0.8	0.8	0.7	0.8	0.7	0.6	0.7	0.6	0.7	0.3	0.7	0.7	-0.2	1.0				
seasonality_std_sm	0.4	0.5	0.5	0.5	0.5	0.4	0.3	0.2	0.2	0.2	0.3	0.4	0.5	0.2	0.3	-0.2	0.2	0.1	0.4	0.5	0.4	0.2	0.5	0.2	1.0			
seasonality_std_tmi	0.6	0.6	0.6	0.6	0.5	0.5	0.5	0.5	0.5	0.5	0.6	0.6	0.6	0.6	0.5	0.1	0.5	0.5	0.6	0.7	0.6	0.6	0.1	0.7	0.5	1.0		
trend_mar2jun	1.0	1.0	1.0	1.0	1.0	1.0	1.0	1.0	1.0	1.0	1.0	1.0	1.0	1.0	1.0	1.0	1.0	1.0	1.0	1.0	1.0	1.0	-0.8	0.2	-0.3	-0.1	1.0	
trend_mar2sep	1.0	1.0	1.0	1.0	1.0	1.0	1.0	1.0	1.0	1.0	1.0	1.0	1.0	1.0	1.0	1.0	1.0	1.0	1.0	1.0	1.0	1.0	-0.4	-0.3	-1.0	-0.4	1.0	1.0

Mask: We produced two raster surfaces for our study area that users can apply for masking any analysis. These masks were intended to define pixels with special conditions where soil will likely not support vegetation or have appropriate soil-climate attributes derived from our models. Our first mask was intended to identify pixels corresponding to ridges, rock outcrops, perennial snow/ice, open water, and developed and barren lands (Figure S6). We defined ridges and rock outcrops by using a combination of topographic position index landforms with a value greater than one standard deviation [classified as a ridge; 91], a topographic slope greater than 35 degrees, and fraction bare ground cover [13] greater than 50%, and tree canopy cover [18] less than 30%. We selected the threshold values and data by examining known rock outcrops, ridges, and cliffs. Using the National land cover database [92] data product, we extracted perennial snow/ice, open water, and developed and barren lands and then added these to the mask. Water bodies larger than 14,00 m^2 (16 pixels) identified from the high resolution, National hydrology dataset [17] were also masked. We also identified pixels assigned no data values in the Polaris soils data [6]. We corrected any missing data within Polaris for our modeling using Esri® ArcGIS™ [24] Nibble™ geoprocessing tool in the Spatial Analyst™ extension by replacing no data values within AWC using a pixel value from its nearest neighbor. However, we created a mask of these values in the event data users prefer to not rely on soil-climate results at these

pixels. We excluded the masks from the soil-climate data products in the event data users prefer to update or produce masks with better or more recent information.

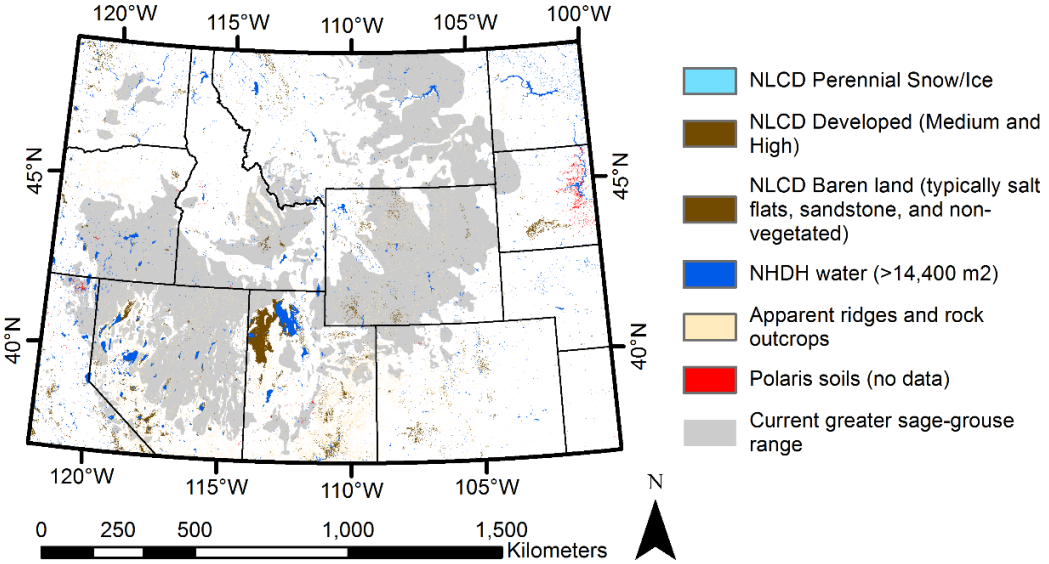

Figure S6. Soil-climate data product mask created for data users to mask pixels in future analyses. The soil-climate data products were produced from our implementation of the Newhall simulation modeling framework applied to the western United States from 1981 to 2010. These pixels were intended to represent features that will not have vegetation or soil. NLCD = National land cover database; NHDH = National hydrography dataset high resolution.

S13. Comparison of soil temperature and moisture regimes between multiple sources

Our modeled soil temperature and moisture regimes (STMR) relied on dynamic climate data and Polaris soil data [6,7]. We compared our STMR products to two independent products, understanding that data and methods for developing those products varied. The first product is a composite of STATSGO2 and gSSURGO developed by Maestas, Campbell, Chambers, Pellant and Miller [9], where they defined soil temperature and moisture regimes to assist land managers with understanding ecosystem functions as they relate to soils and resistance and resilience concepts [93-96]. Second, we assessed gNATSGO because Maestas, Campbell, Chambers, Pellant and Miller [9] did not include our entire study area. Descriptions of USDA and Polaris soil data are provided in section S1. We used the USDA "Soil Data Development Toolbox" [97] to work with the gridded soils data (gNATSGO) and relationship tables depicting soil temperature and moisture. Due to the lack of information on STMR within these data, we also examined a classification associated with any soil component (versus predominate soil component) for a given map unit to maximize data inclusion. However, these two different approaches did not yield the inclusion of additional data, so we decided to use the dominant soil condition derived from "Soil Data Development Toolbox".

We determined the data comparison was problematic due to differences outlined here, but the comparison showed important similarities, so we provided a visual assessment. With the gNATSGO data, the soil moisture and moisture subclasses predominantly lacked classifications but included temperature. The soil-climate regimes defined in USDA were based on soil surveys

dating back to the 1950s, but no information was available on how and when temperature and moisture were collected or associated with survey units. We also determined insufficient details existed on how STMRs were defined from USDA soils using the resistance and resilience data [9]. Therefore, we did not provide a quantitative comparison between products due to significant differences in mapped extents, undocumented methods, and a general lack of information for a meaningful assessment. However, we have provided a visual comparison and discussion of some notable differences between products below.

The three mapped products of soil temperature (Figure S7) and soil moisture (Figure S8) illustrate similarities and differences. All three products use a version of the NRCS soil data, and these figures demonstrate the issues surrounding unmapped soils. When comparing soil temperature of resistance and resilience data to gNATSGO (Figure S7), we observed a lack of mapped information for gNATSGO (missing data), but mostly agreement. We also observed sharp, unrealistic boundaries between Wyoming and Montana (see Figure 1 in main manuscript for state references), which tend to occur in the NRCS data due to differences in how soil scientists classify soils [e.g., 6,7]. When we compared these two products to our soil-climate products, the soil temperature was similar, but our products suggested a replacement of Frigid with Cryic soils, predominately in high plateaus of rangelands. Additionally, we observed in our products slightly warmer temperatures (Frigid) in some foothills of Wyoming mountain ranges, for example, which are likely the effects of snow insulation and spring snowmelt. We also detected much colder temperatures (Pergelic) for mountainous areas at high elevations, likely due to less snow insulating exposed alpine (also not mapped in gNATSGO).

Comparing three mapped soil moisture products (Figure S8) was more challenging. The first notable differences between the three mapped products are the lack of data on soil moisture in gNATSGO. Generally speaking, we illustrate similarities in soil moisture across all three products, but a significant difference occurs in Montana, where our soil-climate products mapped dryer soils compared to the moist estimates classified in the resistance and resilience product. These areas reflect sagebrush-dominated vegetation communities with grasslands near the eastern portion of our study area, but our soil-climate products seemed more consistent with mapping similar soil moisture across associated sagebrush communities.

We also investigated the explanatory power between modeled soil-climate results and ecosystem conditions (sagebrush cover, exposed bare ground, annual herbaceous plant cover, and fire frequency). We reported statistical relationships using generalized additive models to demonstrate correlations between our continuous soil-climate products with sagebrush cover, bare ground cover, herbaceous annual cover (cheatgrass) (Table S9), and burn frequency [1984 – 2016; Landsat burned area essential climate variable [BAECV]; 15; Table S10]. We used generalized additive models to test relations of ecological patterns by assessing the explanatory value of soil temperature-moisture regimes (STMRs), and seasonal soil moisture estimates (i.e., predictors) using variance explained from response variables of sagebrush cover, bare ground, herbaceous annual plant cover, and burn frequency (Table S11).

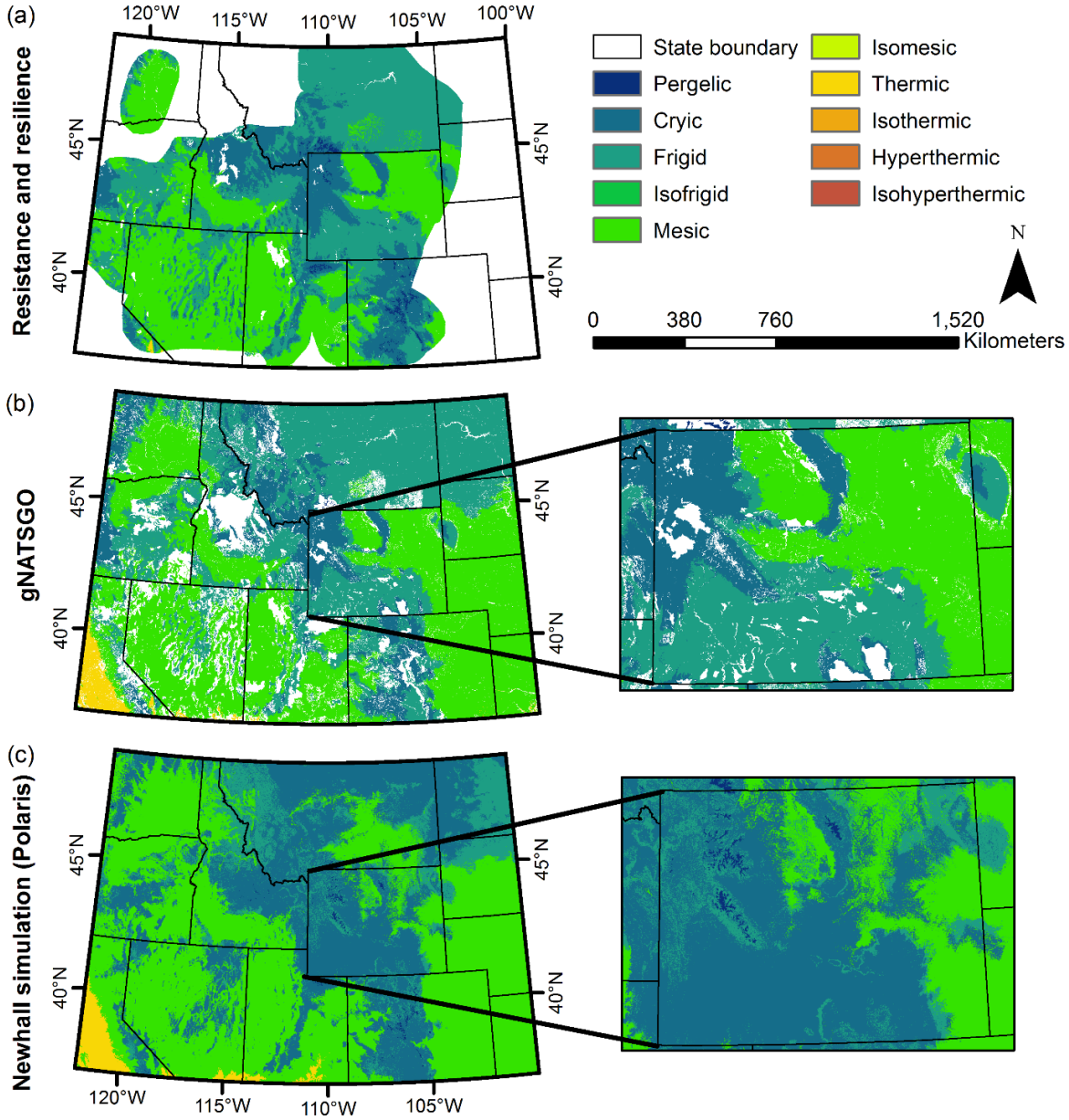

Figure S7. Comparisons of soil temperature regimes defined from those compiled from the U.S. Department of Agriculture (USDA) and our modeled Newhall results. The first dataset (a) included a composite of the state soil geographic database (STATSGO2) and a gridded soil survey geographic database (gSSURGO) developed by Maestas, Campbell, Chambers, Pellant and Miller [9]. This product used soil temperature and moisture characteristics to describe resistance and resilience concepts of the sagebrush biome. The second dataset gNATSGO (b), which relies on gSSURGO and uses STATSGO for a few incomplete mapped areas, is the most current and complete USDA soil data. The third dataset (c) describes what we produced using dynamic climate data (1981 – 2010), Polaris soil data [6,7], and the Newhall simulation model.

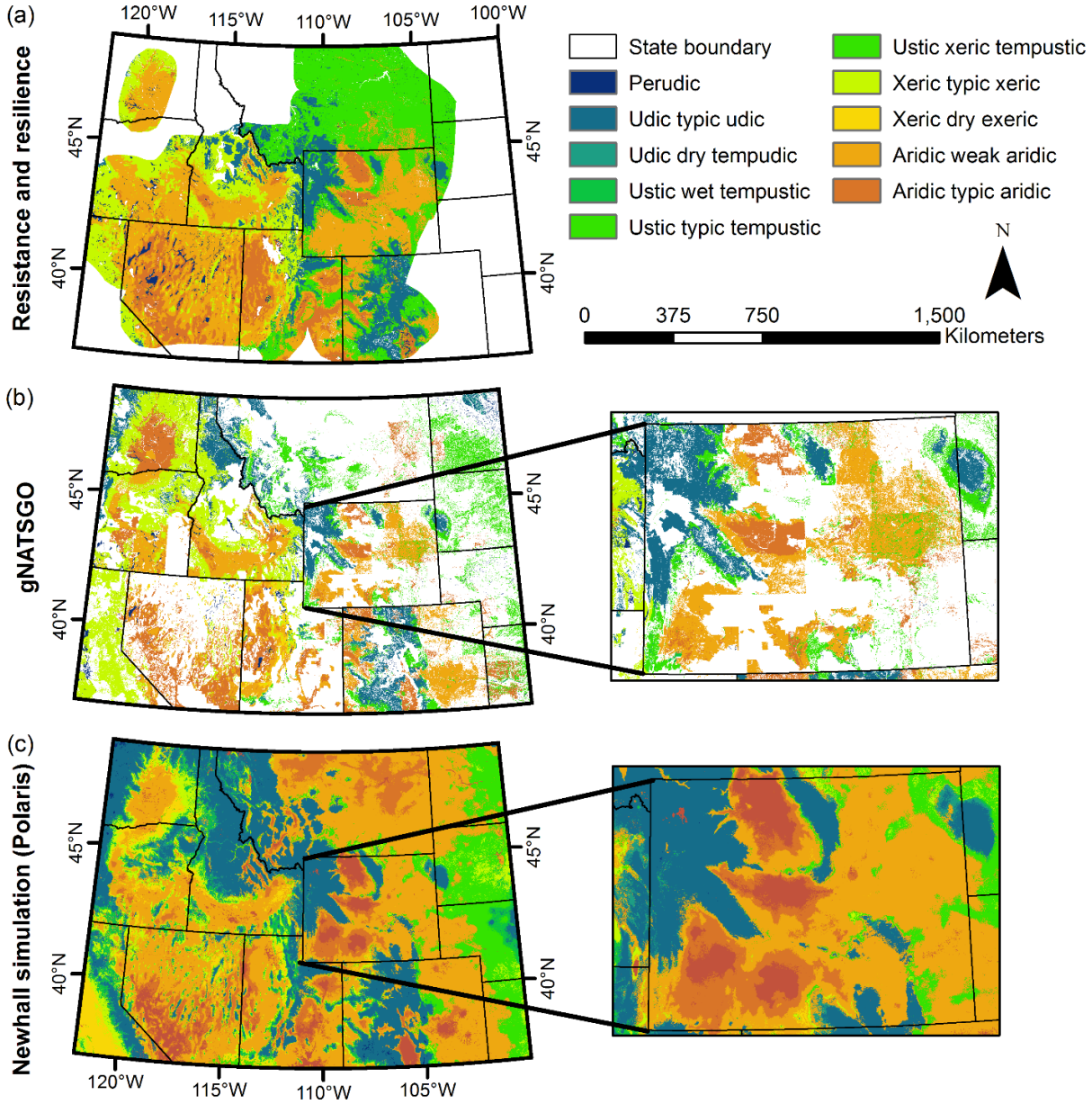

Figure S8. Comparisons of soil moisture regimes defined from those compiled from the U.S. Department of Agriculture (USDA) and our modeled Newhall results. The first dataset (a) included a composite of the state soil geographic database (STATSGO2) and a gridded soil survey geographic database (gSSURGO) developed by Maestas, Campbell, Chambers, Pellant and Miller [9]. This product used soil temperature and moisture characteristics to describe resistance and resilience concepts of the sagebrush biome. The second dataset gNATSGO (b), which relies on gSSURGO and uses STATSGO for a few incomplete mapped areas, is the most current and complete USDA soil data. The third dataset (c) describes what we produced using dynamic climate data (1981 – 2010), Polaris soil data [6,7], and the Newhall simulation model.

Table S9. Top models for annual herbaceous plant cover (A), sagebrush cover (B), and exposed bare ground (C), respectively, predicted using seasonal soil moisture estimates from *spatial_nsm* in generalized additive models. Annual herbaceous cover [16]; sagebrush cover and exposed bare ground provided [13]. 'Mar-Sep*' is a seasonal trend in monthly soil moisture estimate (Theil-Sen slope, March through September). Intercept and coefficient values were calculated using non-transformed data to accurately represent effect sizes, all other statistics are from models with log-transformed response variables. Abbreviations: DE, deviance explained (%); GCV, generalized coefficient of variation; edf, estimated degrees of freedom (an indication of complexity of spline surface); k-index, indicator of spline fit; w_i, Akaike Information Criterion (AIC) weights; Int, Intercept; Co, Coefficient.

A.

				Predictor		X-Y tensile spline					
Predictor	**R^2**	**DE**	**w_i**	**p-value**		**p-value**		**edf**	**k-index**	**Int**	**Co**
Spring s.m.	0.684	68.7	1.0	<0.0001	***	<0.0001	***	1303	0.95	18.8	-0.022
Summer s.m.	0.684	68.7	1.6×10^{-23}	<0.0001	***	<0.0001	***	1326	0.93	17.3	-0.025
Winter s.m.	0.684	68.6	2.3×10^{-44}	<0.0001	***	<0.0001	***	1302	0.94	18.5	-0.026

B.

					Predictor 1		Predictor 2		X-Y tensile spline						
Predictor	**Predictor 2**	**R^2**	**DE**	**w_i**	**p-value**		**p-value**		**p-value**		**edf**	**k-index**	**Int**	**Co 1**	**Co 2**
Spring s.m.	Summer s.m.	0.511	51.5	1.0	<0.0001	***	<0.0001	***	<0.0001	***	1850	1	1.08	0.075	-0.075
Annual s.m.	Mar-Sep*	0.510	51.3	7.8×10^{-253}	<0.0001	***	<0.0001	***	<0.0001	***	1855	0.94	2.08	-0.007	-0.255
Spring s.m.	Autumn s.m.	0.509	51.2	0.0	<0.0001	***	<0.0001	***	<0.0001	***	1856	0.98	2.54	0.052	-0.059

C.

					Predictor 1		Predictor 2		X-Y tensile spline						
Predictor	**Predictor 2**	**R^2**	**DE**	**w_i**	**p-value**		**p-value**		**p-value**		**edf**	**k-index**	**Int**	**Co 1**	**Co 2**
Spring s.m.	Autumn s.m.	0.656	65.9	1.0	<0.0001	***	<0.0001	***	<0.0001	***	1852	0.97	55.51	-0.162	0.159
Mar-Sep*	--	0.656	65.8	2.3×10^{-97}	<0.0001	***	--		<0.0001	***	1850	0.95	56.97	0.751	--
Spring s.m.	Winter s.m.	0.656	65.8	4.4×10^{-147}	<0.0001	***	<0.0001	***	<0.0001	***	1847	0.97	50.20	-0.208	0.198

Table S10. Top models for fire frequency in sagebrush between 1981 and 2015 using seasonal soil moisture estimates as predictors in generalized additive models with a tensile spline smoothing term. Seasonal soil moisture estimates from *spatial_nsm* predict remote sensing derived burn estimates [15]. 'Mar-Sep*' is a seasonal trend in monthly soil moisture estimate (Theil-Sen slope, March through September). Abbreviations: DE, deviance explained (%); GCV, generalized coefficient of variation; edf, estimated degrees of freedom (an indication of complexity of spline surface); k-index, indicator of spline fit; w_i, Akaike Information Criterion (AIC) weights; Int, Intercept; Co, Coefficient.

					Predictor 1		**Predictor 2**		**X-Y tensile spline**						
Predictor	**Predictor 2**	**R^2**	**DE**	**w_i**	**p-value**		**p-value**		**p-value**		**edf**	**k-index**	**Int**	**Co 1**	**Co 2**
Spring s.m.	Autumn s.m.	0.343	34.6	1.0	<0.0001	***	<0.0001	***	<0.0001	***	1728	0.94	0.119	0.00122	-0.00135
Annual s.m.	Mar-Sep*	0.342	34.6	5.7×10^{-14}	<0.0001	***	<0.0001	***	<0.0001	***	1737	0.95	0.113	-0.00013	-0.00560
Summer s.m.	Mar-Sep*	0.342	34.6	1.3×10^{-14}	<0.0001	***	<0.0001	***	<0.0001	***	1737	0.95	0.110	-0.00012	-0.00555
Spring s.m.	Mar-Sep*	0.342	34.6	3.2×10^{-22}	<0.0001	***	<0.0001	***	<0.0001	***	1728	0.94	0.112	-0.00012	-0.00586
Mar-Sep*	--	0.342	34.6	1.9×10^{-22}	<0.0001	***	--		<0.0001	***	1937	0.96	0.112	-0.00520	--

Table S11. Results of statistical models associating soil-climate with ecosystem conditions. Dominant vegetation types were identified using combined Landfire existing vegetation types *[12]*, summarized from the most common associations (based on percent). Soil temperature and moisture regimes (STMR) were created with *spatial_nsm* software, climate normals (1981 – 2010), and soils data across the western United States. Statistical model coefficient estimates identified associations between soil-climate taxonomic classes and three remotely sensed products that characterize habitat conditions in the sagebrush ecosystem: sagebrush cover and exposed bare ground [13] and cover of annual herbaceous plants [known to be strongly influenced by annual *Bromes*; 16*]*. Bolded values indicate statistically significant results (p-value < 0.05).

Common name[1]	**STMR[2]**	**Area (Ha)**	**Dominant vegetation associations (adapted from Landfire 2.0)[3]**	**Sage estimate**	**Pr(>|t|)**	**Ann. herb. estimate**	**Pr(>|t|)**	**Bare estimate**	**Pr(>|t|)**
	Intercept			4.14	**<0.0001**	17.42	**<0.0001**	48.16	**<0.0001**
Frozen Saturated	Pergellic Perudic	25,794	Alpine bedrock and scree, G&I, alpine turf, subalpine forest	2.41	0.3811	--[4]	--	1.54	0.8389
Frozen Very Wet-w4	Pergelic Wet Udic	523,658	Alpine bedrock and scree, alpine turf, G&I, cliff, subalpine meadow	0.17	0.8020	-6.19	0.4150	9.12	**<0.0001**

Common name[1]	STMR[2]	Area (Ha)	Dominant vegetation associations (adapted from Landfire 2.0)[3]	Sage estimate	Pr(>|t|)	Ann. herb. estimate	Pr(>|t|)	Bare estimate	Pr(>|t|)
Frozen ExtremeDry	Pergelic Extreme Aridic	5,935	Alpine bedrock and scree, alpine turf, mt. sage steppe, chaparral	-1.37	0.7731	--	--	2.38	0.8556
Very Cold Saturated	Cryic Perudic	132,844	Spruce-fir F&W, alpine bedrock and scree, G&I, hemlock-silver fir	2.05	**0.0420**	-4.97	0.5041	-3.44	0.2145
Very Cold Very Wet-w4	Cryic Wet Udic	23,804,646	Mt. sage steppe, spruce-fir F&W, lodgepole pine forest, aspen F&W, Douglas-fir F&W	2.88	**<0.0001**	-4.85	**0.0143**	-15.63	**<0.0001**
Very Cold Very Wet-w3	Cryic Typic Udic	232,080	Mt. mixed conifer forest, mt. sage steppe, mt. oak and mixed shrubs, aspen F&W, ponderosa pine F&W	3.10	**<0.0001**	-6.43	**0.0061**	-19.23	**<0.0001**
Very Cold Very Wet-w2	Cryic Dry Tempudic	640,095	Mt. sage steppe, mt. mixed conifer forest, aspen F&W, mt. oak and mixed shrubs, mt. grassland	**4.51**	**<0.0001**	-5.65	**0.0088**	-18.69	**<0.0001**
Very Cold Very Wet-w1	Cryic Dryer Tempudic	2,207,222	Mt. sage steppe, mt. mixed conifer forest, ponderosa pine woodland, aspen F&W	**4.94**	**<0.0001**	-4.71	**0.0195**	-18.34	**<0.0001**
Very Cold Dry-w4	Cryic Weak Xeric	449,544	Mt. sage steppe, low sage steppe, mt. grassland, big sage steppe and shrubland	**4.32**	**<0.0001**	-2.09	0.3039	-11.28	**<0.0001**
Very Cold Dry-w3	Cryic Typic Xeric	772,576	Low sage steppe, mt. sage steppe, big sage shrubland and steppe, juniper woodland	3.80	**<0.0001**	-1.36	0.5012	-9.09	**<0.0001**
Very Cold Dry-w2	Cryic Dry Xeric	1,880,026	Big sage shrubland and steppe, low sage steppe, pasture and crop	1.85	**<0.0001**	-1.67	0.3991	-3.47	0.0006
Very Cold Very Dry-w4	Cryic Weak Aridic	33,637,819	Mixedgrass prairie, big sage steppe and shrubland, mt. sage steppe, crop	3.53	**<0.0001**	-1.32	0.5028	-8.81	**<0.0001**
Very Cold Very Dry-w3	Cryic Typic Aridic	9,017,330	Big sage shrubland and steppe, mixedgrass prairie, crop	2.14	**<0.0001**	-0.43	0.8255	-3.67	0.0001
Very Cold Very Dry-w2	Cryic Dry Aridic	990,199	Big sage shrubland and steppe, semi-desert shrub steppe, saltbush shrubland, greasewood flat	--	--	--	--	--	--

Common name[1]	STMR[2]	Area (Ha)	Dominant vegetation associations (adapted from Landfire 2.0)[3]	Sage estimate	Pr(>|t|)	Ann. herb. estimate	Pr(>|t|)	Bare estimate	Pr(>|t|)
Very Cold ExtremeDry	Cryic Extreme Aridic	1,759,260	Big sage shrubland and steppe, crop and pasture, saltbush shrubland, greasewood flat	1.00	**0.0108**	-0.12	0.9519	-1.92	0.0746
Cold Saturated	Frigid Perudic	66,769	Spruce-fir F&W, Alpine bedrock and scree, hemlock-silver fir forest, G&I, hemlock forest	1.94	0.4828	--	--	-15.53	0.0410
Cold Very Wet-w4	Frigid Wet Udic	14,886,595	Lodgepole pine forest, spruce-fir F&W, mt. mixed conifer forest, Douglas-fir F&W	2.32	**<0.0001**	-5.73	0.0044	-15.37	**<0.0001**
Cold Very Wet-w3	Frigid Typic Udic	194,514	Mt. mixed conifer forest, lodgepole pine forest, ponderosa pine woodland, Douglas-fir F&W	3.09	**0.0024**	-10.31	0.0176	-19.64	**<0.0001**
Cold Very Wet-w2	Frigid Dry Tempudic	288,923	Mt. mixed conifer forest, Douglas-fir forest, lodgepole pine forest, ponderosa pine woodland	4.62	**<0.0001**	-3.66	0.6043	-22.08	**<0.0001**
Cold Very Wet-w1	Frigid Dryer Tempudic	684,717	Mt. mixed conifer, ponderosa pine woodland, mt. mixed conifer, mt. Douglas-fir F&W, aspen F&W	3.58	**<0.0001**	-1.33	0.6776	-19.92	**<0.0001**
Cold Wet-w4	Frigid Wet Tempustic	777,983	Mt. mixed conifer forest, mt. sage steppe, ponderosa pine woodland, low sage steppe, mt. Douglas-fir F&W	4.02	**<0.0001**	-2.56	0.2229	-15.51	**<0.0001**
Cold Wet-w3	Frigid Typic Tempustic	7,811,500	Mixedgrass prairie, crop and pasture, grassland	3.13	**<0.0001**	-0.91	0.6481	-11.75	**<0.0001**
Cold Dry-w4	Frigid Weak Xeric	703,472	Mt. sage steppe, pinyon-juniper woodland, big sage shrubland and steppe, mixed-grass prairie, low sage steppe	4.99	**<0.0001**	-1.28	0.5268	-13.02	**<0.0001**
Cold Dry-w3	Frigid Typic Xeric	1,390,110	Big sage shrubland and steppe, mixedgrass prairie, mt. sage steppe, crop	3.42	**<0.0001**	-0.95	0.6336	-9.12	**<0.0001**
Cold Dry-w2	Frigid Dry Xeric	2,101	Ponderosa pine woodland, pasture, mt. mixed conifer, mt. deciduous shrub	8.11	**0.0858**	--	--	-19.07	0.1409
Cold Very Dry-w4	Frigid Weak Aridic	4,699,032	Mixedgrass prairie, big sage steppe and shrubland, crop and pasture	2.89	**<0.0001**	-0.22	0.9111	-6.93	**<0.0001**

Common name[1]	STMR[2]	Area (Ha)	Dominant vegetation associations (adapted from Landfire 2.0)[3]	Sage estimate	Pr(>|t|)	Ann. herb. estimate	Pr(>|t|)	Bare estimate	Pr(>|t|)
Cold Very Dry-w3	Frigid Typic Aridic	764,780	Mixedgrass prairie, big sage steppe and shrubland, crop and pasture	2.24	**<0.0001**	0.28	0.8884	-2.86	0.0062
Cold Very Dry-w2	Frigid Dry Aridic	46,519	Big sage shrubland, xeric mixed sage, pinyon-juniper woodland, pasture	3.40	***0.0007***	-1.65	0.5907	-8.00	0.0038
Cold ExtremeDry	Frigid Extreme Aridic	219,399	Big sage shrubland, saltbush shrubland, big sage steppe, crop	0.59	0.3129	-1.59	0.4696	-0.04	0.9799
Warm Saturated	Mesic Perudic	3,597	Hemlock-silver fir forest, hemlock forest, silver fir-hemlock-Douglas fir forest, subalpine turf, bedrock						
Warm Very Wet-w4	Mesic Wet Udic	7,586,488	Mt. mixed conifer forest, hemlock-silver fir forest, ponderosa pine woodland, sand prairie, Med. mixed conifer F&W	3.21	**<0.0001**	-5.56	**0.0067**	-16.71	**<0.0001**
Warm Very Wet-w3	Mesic Typic Udic	262,470	Mt. mixed conifer F&W, ponderosa pine woodland, Med. mixed conifer woodland	3.46	**0.0017**	-9.25	**0.0338**	-20.90	**<0.0001**
Warm Very Wet-w2	Mesic Dry Tempudic	788,865	Mt. mixed conifer forest, ponderosa pine woodland, Med. mixed conifer woodland, mt. deciduous shrubland	5.28	**<0.0001**	-6.78	**0.0063**	-14.72	**<0.0001**
Warm Very Wet-w1	Mesic Dryer Tempudic	2,138,783	Mt. mixed conifer forest, ponderosa pine woodland, mt. deciduous shrubland, mt. sage steppe	3.53	**<0.0001**	-5.13	**0.0135**	-14.83	**<0.0001**
Warm Wet-w4	Mesic Wet Tempustic	10,256,382	Sand prairie, mt. sage steppe, pinyon-juniper woodland, ponderosa pine woodland, mt. mixed conifer F&W	4.77	**<0.0001**	-4.53	**0.0221**	-13.13	**<0.0001**
Warm Wet-w3	Mesic Typic Tempustic	15,412,809	Mixedgrass prairie, sand prairie, crop, shortgrass prairie	2.91	**<0.0001**	-0.90	0.6490	-6.85	**<0.0001**
Warm Dry-w4	Mesic Weak Xeric	4,403,682	Crop, mixedgrass prairie, big sage shrubland and steppe, mt. sage steppe	4.32	**<0.0001**	-2.99	0.1325	-11.31	**<0.0001**
Warm Dry-w3	Mesic Typic Xeric	7,739,982	Big sage shrubland and steppe, mixedgrass prairie, crop, pinyon-juniper woodland, mt. sage steppe	3.97	**<0.0001**	-2.18	0.2688	-8.54	**<0.0001**

Common name[1]	STMR[2]	Area (Ha)	Dominant vegetation associations (adapted from Landfire 2.0)[3]	Sage estimate	Pr(>|t|)	Ann. herb. estimate	Pr(>|t|)	Bare estimate	Pr(>|t|)
Warm Dry-w2	Mesic Dry Xeric	4,198,321	Big sage shrubland and steppe, crop, grassland steppe, pinyon-juniper woodland, introduced annual grassland	2.60	**<0.0001**	0.19	0.9228	-5.21	**<0.0001**
Warm Very Dry-w4	Mesic Weak Aridic	58,110,776	Big sage shrubland and steppe, shortgrass prairie, mixedgrass prairie, crop, pinyon-juniper woodland	1.69	**<0.0001**	-0.18	0.9275	-2.42	0.0128
Warm Very Dry-w3	Mesic Typic Aridic	8,610,253	Big sage shrubland, salt desert scrub, playa, xeric mixed sage, semi-desert steppe, mixed desert scrub, greasewood flat	-0.08	0.8322	-0.32	0.8699	2.76	**0.0047**
Warm Very Dry-w2	Mesic Dry Aridic	348,117	Salt desert scrub, big sage shrubland, semi-desert steppe, greasewood flat, crop	0.30	0.5466	3.29	0.1200	1.15	0.3980
Warm Extreme Dry	Mesic Extreme Aridic	4,945,022	Greasewood flat, mixed desert scrub, salt-desert scrub, shortgrass prairie, big sage shrubland, playa	-0.94	**0.0098**	-0.04	0.9828	3.98	**0.0001**
Hot Wet-w4	Thermic Wet Tempustic	52,968	Coastal and Med. oak woodland, Med. conifer F&W, coastal redwood forest, grassland, chaparral	3.49	0.1618	--	--	-10.39	0.1287
Hot Wet-w3	Thermic Typic Tempustic	366,806	Mixed desert scrub, creosote-bursage scrub, warm desert scrub and shrub, grassland, pinyon-juniper woodland	0.62	0.3939	-1.09	0.6284	1.48	0.4605
Hot Dry-w4	Thermic Weak Xeric	163,442	Med. conifer F&W, chaparral, grassland, Med. mixed oak woodland, mt. pine woodland	3.06	**0.0536**	--	--	3.70	0.3951
Hot Dry-w3	Thermic Typic Xeric	593,679	Ruderal grassland, mt. pine woodland, Med. conifer F&W, Med. mixed oak woodland, chaparral, coastal oak woodland	2.23	**0.0165**	--	--	-6.77	**0.0081**
Hot Dry-w2	Thermic Dry Xeric	3,404,865	Ruderal grassland, crop, developed, mt. pine woodland	1.19	**0.0607**	0.47	0.8392	-2.12	0.2231

Common name[1]	STMR[2]	Area (Ha)	Dominant vegetation associations (adapted from Landfire 2.0)[3]	Sage estimate	Pr(>|t|)	Ann. herb. estimate	Pr(>|t|)	Bare estimate	Pr(>|t|)
Hot Very Dry-w4	Thermic Weak Aridic	247,756	Mixed desert scrub, blackbrush-ephedra shrubland, creosote-bursage scrub, bedrock, cliff, salt desert scrub	-0.29	0.6231	-0.71	0.7446	1.79	0.2651
Hot Very Dry-w3	Thermic Typic Aridic	1,983	Bedrock canyon and tableland, blackbrush-ephedra shrubland, mixed desert scrub, creosote-bursage scrub	--	--	--	--	--	--
Hot Extreme Dry	Thermic Extreme Aridic	452,439	Bedrock canyon and tableland, blackbrush-ephedra shrubland, creosote-bursage scrub, mixed desert scrub, bedrock	-2.18	**0.0046**	-1.08	0.6931	6.08	**0.0040**
Hot Wet-w3	Isothermic Typic Tempustic	1,069	Coastal redwood forest, coastal oak woodland, urban forest, coastal conifer F&W	--	--	--	--	--	--

[1]Abbreviations: To simplify 'Common name' labels, we indicate moisture subdivisions (wetter to drier) using the notation w4 (wet), w3 (typic), w2 (dry), and w1 (dryer).

[2]Omitted STMR classes: These exist in model output but omitted here due to *small areal size* (<1000 acres) within study area. Vegetation associations and statistics could not be meaningfully determined for the following STMR classes: isomesic temperature regime with dry tropudic, dryer tropudic, typic tempustic, typic tropustic, udic tropustic, and extreme aridic moisture regimes; thermic temperature regime with wet udic, typic udic dry tempudic, dryer tempudic moisture regimes; isothermic temperature regime with dryer tropudic, typic tropustic, udic tropustic and extreme aridic moisture regimes; and thermic temperature with dry aridic soil moisture.

[3]Abbreviations: annual herbaceous plants (Ann. Herb); bedrock and scree (B&S), may include cliff and talus and agricultural crops; glacier and ice field (G&I); Mediterranean (Med.); montane (mt.); dominated/co-dominated sagebrush species (sage); forest and woodland (F&W).

[4]Statistical fields with no data (i.e., habitat conditions that do not overlap soil-climate data) denoted as '--'.

References

1. Prism Climate Group. Precipitation and temperature climate normals (1981 – 2010). Oregon State University, available at http://prism.oregonstate.edu, Accessed 20 Dec. 2017, 2015.
2. U.S. Department of Agriculture, N.R.C.S. Soil climate analysis network (SCAN). Available at https://www.wcc.nrcs.usda.gov/scan/. Accessed 9 Apr. 2020, 2020.
3. Dorigo, W.; Himmelbauer, I.; Aberer, D.; Schremmer, L.; Petrakovic, I.; Zappa, L.; Preimesberger, W.; Xaver, A.; Annor, F.; Ardö, J., et al. The International Soil Moisture Network: serving Earth system science for over a decade. *Hydrology and Earth System Sciences* **2021**, *25*, 5749-5804, doi:10.5194/hess-25-5749-2021.
4. Arguez, A.; Durre, I.; Applequist, S.; Squires, M.F.; Vose, R.S.; Yin, X.; Bilotta, R. NOAA's U.S. Climate Normals (1981-2010). NOAA National Centers for Environmental Information, A.J., Ed. 2010; 10.7289/V5PN93JP.
5. National Operational Hydrologic Remote Sensing Center. Snow Data Assimilation System (SNODAS) Data Products at NSIDC, Version 1. Boulder, Colorado USA. NSIDC: National Snow and Ice Data Center. https://doi.org/10.7265/N5TB14TC, 2004.
6. Chaney, N.W.; Minasny, B.; Herman, J.D.; Nauman, T.W.; Brungard, C.W.; Morgan, C.L.S.; McBratney, A.B.; Wood, E.F.; Yimam, Y. POLARIS soil properties: 30-m probabilistic maps of soil properties over the contiguous United States. *Water Resources Research* **2019**, *55*, 2916-2938, doi:10.1029/2018wr022797.
7. Chaney, N.W.; Wood, E.F.; McBratney, A.B.; Hempel, J.W.; Nauman, T.W.; Brungard, C.W.; Odgers, N.P. POLARIS: a 30-meter probabilistic soil series map of the contiguous United States. *Geoderma* **2016**, *274*, 54-67, doi:10.1016/j.geoderma.2016.03.025.
8. Soil Survey Staff. Gridded national soil survey geographic (gNATSGO) database (July 2020 source). United States Department of Agriculture, Natural Resources Conservation Service. Available online at https://nrcs.app.box.com/v/soils. Accessed 5 Apr. 2021, 2020.
9. Maestas, J.D.; Campbell, S.B.; Chambers, J.C.; Pellant, M.; Miller, R.F. Tapping soil survey information for rapid assessment of sagebrush ecosystem resilience and resistance. *Rangelands* **2016**, *38*, 120-128, doi:10.1016/j.rala.2016.02.002.
10. U.S. Geological Survey. 1/3rd arc-second digital elevation models (DEMs) - USGS National Map 3DEP downloadable data collection. U.S. Geological Survey, Reston, Virginia, USA. Available at https://www.usgs.gov/core-science-systems/ngp/3dep/about-3dep-products-services. Accessed 4 Apr. 2018.: 2018.
11. Yang, L.; Jin, S.; Danielson, P.; Homer, C.; Gass, L.; Bender, S.M.; Case, A.; Costello, C.; Dewitz, J.; Fry, J., et al. A new generation of the United States National Land Cover Database: Requirements, research priorities, design, and implementation strategies. *ISPRS Journal of Photogrammetry and Remote Sensing* **2018**, *146*, 108-123, doi:10.1016/j.isprsjprs.2018.09.006.
12. U.S. Geological Survey. LANDFIRE Existing Vegetation Type layer version 2.0.0. U.S. Geological Survey, Reston, Virginia, USA. Available at https://www.landfire.gov. Accessed 30 Jan. 2021, 2019.
13. Rigge, M.; Homer, C.; Cleeves, L.; Meyer, D.K.; Bunde, B.; Shi, H.; Xian, G.; Schell, S.; Bobo, M. Quantifying western U.S. rangelands as fractional components with multi-resolution remote sensing and in situ data. *Remote Sensing* **2020**, *12*, 412-412, doi:10.3390/rs12030412.

14. Xian, G.; Homer, C.; Rigge, M.; Shi, H.; Meyer, D. Characterization of shrubland ecosystem components as continuous fields in the northwest United States. *Remote Sensing of Environment* **2015**, *168*, 286-300, doi:10.1016/j.rse.2015.07.014.
15. Hawbaker, T.J.; Vanderhoof, M.K.; Schmidt, G.L.; Beal, Y.-J.; Picotte, J.J.; Takacs, J.D.; Falgout, J.T.; Dwyer, J.L. The landsat burned area algorithm and products for the conterminous United States. *Remote Sensing of Environment* **2020**, *244*, doi:10.1016/j.rse.2020.111801.
16. Maestas, J.; Jones, M.; Pastick, N.J.; Rigge, M.B.; Wylie, B.K.; Garner, L.; Crist, M.; Homer, C.G.; Boyte, S.; Whitacre, B. Annual herbaceous cover across rangelands of the sagebrush biome. U.S. Geological Survey data release, https://doi.org/10.5066/P9VL3LD5, 2020.
17. U.S. Geological Survey. National Hydrology Dataset High Resolution. U.S. Geological Survey, Reston, Virginia, USA, available at https://nhd.usgs.gov/data.html, accessed 20 Dec. 2017: 2017.
18. U.S. Geological Survey. NLCD 2016 U.S. Forest Service percent tree canopy (analytical version). U.S. Geological Survey, Earth Resources Observation and Science, South Dakota, USA, available at https://www.mrlc.gov/, accessed 04 Jan. 2018: 2016.
19. Clow, D.W.; Nanus, L.; Verdin, K.L.; Schmidt, J. Evaluation of SNODAS snow depth and snow water equivalent estimates for the Colorado Rocky Mountains, USA. *Hydrological Processes* **2012**, *26*, 2583-2591, doi:10.1002/hyp.9385.
20. Hedrick, A.; Marshall, H.P.; Winstral, A.; Elder, K.; Yueh, S.; Cline, D. Independent evaluation of the SNODAS snow depth product using regional-scale lidar-derived measurements. *The Cryosphere* **2015**, *9*, 13-23, doi:10.5194/tc-9-13-2015.
21. Lv, Z.; Pomeroy, J.W.; Fang, X. Evaluation of SNODAS snow water equivalent in western Canada and assimilation Into a cold region hydrological model. *Water Resources Research* **2019**, *55*, 11166-11187, doi:10.1029/2019wr025333.
22. Zahmatkesh, Z.; Tapsoba, D.; Leach, J.; Coulibaly, P. Evaluation and bias correction of SNODAS snow water equivalent (SWE) for streamflow simulation in eastern Canadian basins. *Hydrological Sciences Journal* **2019**, *64*, 1541-1555, doi:10.1080/02626667.2019.1660780.
23. Hengl, T.; Mendes de Jesus, J.; Heuvelink, G.B.; Ruiperez Gonzalez, M.; Kilibarda, M.; Blagotic, A.; Shangguan, W.; Wright, M.N.; Geng, X.; Bauer-Marschallinger, B., et al. SoilGrids250m: Global gridded soil information based on machine learning. *PLoS One* **2017**, *12*, e0169748, doi:10.1371/journal.pone.0169748.
24. Environmental Systems Research Institute. ArcGIS Desktop. Version 10.7.1. Environmental Systems Research Institute: Redlands, 2011.
25. Soille, P. Optimal removal of spurious pits in grid digital elevation models. *Water Resources Research* **2004**, *40*, 1-9, doi:10.1029/2004WR003060.
26. Tarboton, D.; Bras, R.; Rodriguez-Iturbe, I. On the extraction of channel networks from digital elevation data. *Hydrological Processes* **1991**, *5*, 81-100, doi:10.1002/hyp.3360050107.
27. McCune, B.; Keon, D. Equations for potential annual direct incident radiation and heat load. *Journal of Vegetation Science* **2002**, *13*, 603-606, doi:10.1111/j.1654-1103.2002.tb02087.x.

28. Sappington, J.M.; Longshore, K.M.; Thompson, D.B. Quantifying landscape ruggedness for animal habitat analysis: a case study using bighorn sheep in the Mojave Desert. *The Journal of Wildlife Management* **2007**, *71*, 1419-1426, doi:10.2193/2005-723.
29. GDAL/OGR contributors *GDAL/OGR Geospatial Data Abstraction software Library*, Open Source Geospatial Foundation: 2020.
30. Jordahl, K. *GeoPandas: Python tools for geographic data*, 2014.
31. Harris, C.R.; Millman, K.J.; van der Walt, S.J.; Gommers, R.; Virtanen, P.; Cournapeau, D.; Wieser, E.; Taylor, J.; Berg, S.; Smith, N.J., et al. Array programming with NumPy. *Nature* **2020**, *585*, 357-362, doi:10.1038/s41586-020-2649-2.
32. McKinney, W. Data structures for statistical computing in Python. In Proceedings of Proceedings of the 9th Python in Science Conference (SciPy), Austin, Texas, United States; pp. 56-61.
33. Gillies, S.; others, a. *Rasterio: geospatial raster I/O for {Python} programmers*, Available at https://github.com/mapbox/rasterio. Accessed on xx.: 2013.
34. Pedregosa, F.; Varoquaux, G.; Gramfort, A.; Michel, V.; Thirion, B.; Grisel, O.; Blondel, M.; Prettenhofer, P.; Weiss, R.; Dubourg, V., et al. Scikit-learn: machine learning in Python. *Journal of Machine Learning Research* **2011**, *12*, 2825-2830.
35. Virtanen, P.; Gommers, R.; Oliphant, T.E.; Haberland, M.; Reddy, T.; Cournapeau, D.; Burovski, E.; Peterson, P.; Weckesser, W.; Bright, J., et al. SciPy 1.0: fundamental algorithms for scientific computing in Python. *Nat Methods* **2020**, *17*, 261-272, doi:10.1038/s41592-019-0686-2.
36. Gillies, S. *Shapely: manipulation and analysis of geometric objects*, Available at https://github.com/Toblerity/Shapely; Accessed 23 Nov. 2020.: 2007.
37. Seabold, S.; Perktold, J. Statsmodels: econometric and statistical modeling with Python. In Proceedings of Proceedings of the 9th Python in Science Conference (SciPy), Austin, Texas, United States; pp. 92-96.
38. O'Donnell, M.S.; Manier, D.J. *spatial_nsm*: Spatial estimates of soil-climate properties using a modified Newhall simulation model (version 1.0.0). U.S. Geological Survey software release, https://doi.org/10.5066/P97XRNTX: 2022.
39. U.S. Geological Survey Advanced Research Computing. USGS Denali Supercomputer. U.S. Geological Survey, https://doi.org/10.5066/P9PSW367: 2021.
40. Salley, S.W.; Sleezer, R.O.; Bergstrom, R.M.; Martin, P.H.; Kelly, E.F. A long-term analysis of the historical dry boundary for the Great Plains of North America: Implications of climatic variability and climatic change on temporal and spatial patterns in soil moisture. *Geoderma* **2016**, *274*, 104-113, doi:10.1016/j.geoderma.2016.03.020.
41. Winzeler, H.E.; Owens, P.R.; Waltman, S.W.; Waltman, W.J.; Libohova, Z.; Beaudette, D. A methodology for examining changes in soil climate geography through time: U.S. soil moisture regimes for the period 1971-2000. *Soil Science Society of America Journal* **2013**, *77*, 213-225, doi:10.2136/sssaj2012.0123.
42. Smith, G.D.; Newhall, F.; Robinson, L.H.; Swanson, D. Soil temperature regimes, their characteristics and predictability. U.S. Department of Agriculture, Soil Conservation Service, SCS-TP-144 (1964): 1964; pp 1-14.
43. Maurer, G.E.; Bowling, D.R. Seasonal snowpack characteristics influence soil temperature and water content at multiple scales in interior western U.S. mountain ecosystems. *Water Resources Research* **2014**, *50*, 5216-5234, doi:10.1002/2013wr014452.

44. Zhang, Y.; Sherstiukov, A.B.; Qian, B.; Kokelj, S.V.; Lantz, T.C. Impacts of snow on soil temperature observed across the circumpolar north. *Environmental Research Letters* **2018**, *13*, doi:10.1088/1748-9326/aab1e7.
45. Lacelle, D.; Lapalme, C.; Davila, A.F.; Pollard, W.; Marinova, M.; Heldmann, J.; McKay, C.P. Solar radiation and air and ground temperature relations in the cold and hyper-arid Quartermain Mountains, McMurdo dry valleys of Antarctica. *Permafrost and Periglacial Processes* **2016**, *27*, 163-176, doi:10.1002/ppp.1859.
46. Zhang, T. Influence of the seasonal snow cover on the ground thermal regime: an overview. *Reviews of Geophysics* **2005**, *43*, doi:10.1029/2004rg000157.
47. Molga, M. *Agricultural meteorology. 2. Outline of agrometeorological problems*; Centralny Inst. Inform. : Naukowo-Teeh. Ekon., Warsaw (Polish), 1958.
48. Vandeput, N. *Data science for supply chain forecasting*; De Gruyter: 2021.
49. Tofallis, C. A better measure of relative prediction accuracy for model selection and model estimation. *Journal of the Operational Research Society* **2015**, *66*, 1352-1362, doi:10.1057/jors.2014.103.
50. Flores, B.E. A pragmatic view of accuracy measurement in forecasting. *Omega* **1986**, *14*, 93-98, doi:https://doi.org/10.1016/0305-0483(86)90013-7.
51. Abkenar, F.Z.; Rasoulzadeh, A.; Asghari, A. Performance evaluation of different soil water retention functions for modeling of water flow under transient condition. *Bragantia* **2019**, *78*, 119-130, doi:10.1590/1678-4499.2017406.
52. Lytle, D.J.; Bliss, N.B.; Waltman, S.W. Interpreting the State Soil Geographic Database (STATSGO). In *GIS and environmental modeling: progress and research issues*, 1st ed.; Goodchild, M.F., Steyaert, L.T., Parks, B.O., Johnston, C., Maidment, D., Crane, M., Glendinning, S., Eds. John Wiley and Sons, Inc.: New York, USA., 1996; pp. 49 - 52.
53. Thornthwaite, C.W. An approach toward a rational classification of climate. *Geographical Review* **1948**, *38*, 55-94.
54. Berti, A.; Tardivo, G.; Chiaudani, A.; Rech, F.; Borin, M. Assessing reference evapotranspiration by the Hargreaves method in north-eastern Italy. *Agricultural Water Management* **2014**, *140*, 20-25, doi:10.1016/j.agwat.2014.03.015.
55. Allen, R.G.; Pereira, L.S.; Raes, D.; Smith, M. Crop evapotranspiration: Guidelines for computing crop water requirements. In FAO Irrigation and Drainage Paper no. 56. FAO, Rome, 1998.
56. Lu, J.; Sun, G.; McNulty, S.G.; Amatya, D.M. A comparison of six potential evapotranspiration methods for regional use in the southeastern United States. *Journal of the American Water Resources Association* **2005**, 621-633.
57. Sun, X.; Li, J.; Zhou, A. Evaluation and comparison of methods for calculating Thornthwaite moisture index. *Australian Geomechanics* **2017**, *52*, 62-75.
58. Grismer, M.E.; Orang, M.; Snyder, R.; Matyac, R. Pan evaporation to reference evapotranspiration conversion methods. *Journal of Irrigation and Drainage Engineering* **2002**, *128*, 180-184, doi:10.1061/(ASCE)0733-9437(2002)128:3(180).
59. Lang, D.; Zheng, J.; Shi, J.; Liao, F.; Ma, X.; Wang, W.; Chen, X.; Zhang, M. A Comparative study of potential evapotranspiration estimation by eight methods with FAO Penman–Monteith method in southwestern China. *Water* **2017**, *9*, doi:10.3390/w9100734.

60. Grace, B.; Quick, B. A comparison of methods for the calculation of potential evapotranspiration under the windy semi-arid conditions of southern Alberta. *Canadian Water Resources Journal* **1988**, *13*, 9-19, doi:10.4296/cwrj1301009.
61. Fisher, J.B.; Whittaker, R.J.; Malhi, Y. ET come home: potential evapotranspiration in geographical ecology. *Global Ecology and Biogeography* **2011**, *20*, 1-18, doi:10.1111/j.1466-8238.2010.00578.x.
62. Vörösmarty, C.J.; Federer, C.A.; Schloss, A.L. Potential evaporation functions compared on US watersheds: possible implications for global-scale water balance and terrestrial ecosystem modeling. *Journal of Hydrology* **1998**, *207*, 147-169.
63. Zhao, L.; Xu, F.; Xia, J.; Wu, H. Applicability of 12 PET estimation methods in different climate regions in China. *Hydrology Research* **2021**, *52*, 636-657, doi:10.2166/nh.2021.128.
64. Thornthwaite, C.W.; Mather, J.R. The water balance. *Publications in Climatology* **1955**, *8*, 1-104.
65. Sellers, W.D. *Physical climatology*, 4th ed.; University of Chicago Press: 1965.
66. Hargreaves, G.H.; Allen, R.G. History and evaluation of Hargreaves evapotranspiration equation. *Journal of Irrigation and Drainage Engineering* **2003**, *129*, 53-63, doi:10.1061/(ASCE)0733-9437(2003)129:1(53).
67. Hamon, W.R. Estimating Potential Evapotranspiration. *Journal of the Hydraulics Division, Proceedings of the American Society of Civil Engineers* **1961**, *87*, 107-120.
68. Allen, R.G.; Walter, I.A.; Elliott, R.; Howell, T.; Itenfisu, D.; Jensen, M. The ASCE standardized reference evapotranspiration equation. Reston, Va., American Society of Civil Engineers, 2005; p 196.
69. Priestley, C.H.B.; Taylor, R.J. On the assessment of surface heat flux and evaporation using large-scale parameters. *Monthly Weather Review* **1972**, *100*, 81-92.
70. Makkink, G.F. Testing the Penman formula by means of lysimeters. *Journal of the Institution of Water Engineers* **1957**, *11*, 277-288.
71. Oudin, L.; Moulin, L.; Bendjoudi, H.; Ribstein, P. Estimating potential evapotranspiration without continuous daily data: possible errors and impact on water balance simulations. *Hydrological Sciences Journal* **2010**, *55*, 209-222, doi:10.1080/02626660903546118.
72. Thornthwaite, C.W.; Mather, J.R. Instructions and tables for computing potential evapotranspiration and the water balance: Centerton, N.J., Laboratory of Climatology. *Publications in Climatology* **1957**, *10*, 185-311.
73. Black, P.E. Revisiting the Thornthwaite and Mather water balance. *JAWRA Journal of the American Water Resources Association* **2007**, *43*, 1604-1605, doi:10.1111/j.1752-1688.2007.00132.x.
74. Chen, D.; Gao, G.; Xu, C.-Y.; Guo, J.; Ren, G. Comparison of the Thornthwaite method and pan data with the standard Penman-Monteith estimates of reference evapotranspiration in China. *Climate Research* **2005**, *28*, 123-132, doi:10.3354/cr028123.
75. Van Wambeke, A.R. Calculated soil moisture and temperature regimes of Africa. U.S. Department of Agriculture, Soil Management Support Services Technical Monograph No. 3: Washington, District of Columbia, United States, 1982; pp 1-185.
76. Van Wambeke, A.R. The Newhall Simulation Model for estimating soil moisture & temperature regimes. Department of Crop and Soil Sciences: Cornell University, Ithaca, New York, United States, 2000; pp 1-9.

77. Newhall, F.; Berdanier, C.R. Calculation of soil moisture regimes from the climatic record. U.S. Department of Agrisulture, Natural Resources Conservation Service: National Soil Survey Center, Lincoln, Nebraska, United States, 1996; pp 1-15.
78. Newhall, F. Calculation of soil moisture regimes from climatic record. Rev. 4 Mimeographed. U.S. Department of Agriculture, Soil Conservation Service: Washington, DC, United States, 1972; p 17.
79. National Soil Survey Center. Soil quality resource concerns: available water capacity. U.S. Department of Agriculture, Natural Resources Conservation Service: Available at https://www.nrcs.usda.gov/Internet/FSE_DOCUMENTS/nrcs142p2_051279.pdf. Accessed 31 March 2021, 1998; p 2.
80. Rabenhorst, M.C. Biologic zero: A soil temperature concept. *Wetlands* **2005**, *25*, 615-621.
81. Smith, G.D. The Guy Smith Interviews: Rationale for concepts in soil taxonomy. Soil Management Support Services, Soil Conservation Service, United States Department of Agriculture: 1986; pp 1-277.
82. Nimlos, T.J. Rationale for the soil moisture and temperature criteria used in soil taxonomy. *Soil survey horizons* **1987**, *28*, 120-125, doi:10.2136/sh1987.4.0120.
83. Tejedor, M.; Jiménez, C.; Rodríguez, M.; Neris, J. Controversies in the definition of "Iso" soil temperature regimes. *Soil Science Society of America Journal* **2009**, *73*, 983-988, doi:10.2136/sssaj2008.0236.
84. Soil Survey Staff. Soil taxonomy: a basic system of soil classification for making and interpreting soil surveys. second ed.; United States Department of Agriculture, Natural Resources Conservation Service: 1999; p 886.
85. Paetzold, R.F. Soil climate definitions used in soil taxonomy. In *Proceedings of the fourth international Soil Correlation Meeting (ISCOM IV): characterization, classification, and utilization of aridisols. Part A. Papers.*, Kimble, J.M., Nettleton, W.D., Eds. U.S. Department of Agriculture, Soil Conservation Service: Lincoln, Nebraska, 1990; pp. 151-166.
86. Wilcox, J.C.; Sly, W.K. Use of negative values of potential evapotranspiration in estimation of annual irrigation requirements. *Canadian Journal of Soil Science* **1976**, *56*, 507-509, doi:10.4141/cjss76-061.
87. Billaux, P. The soil moisture regime estimated by means of climate data, its relationships with annual rainfall and with bioclimatic classifications under mediterranean climate conditions. The Arab Center for the Studies of Arid Zone and Dry Lands, First training course in agrometeorology for arid zones, 10-23 May 1982: Damascus, Syria, 1982; pp 1-28.
88. U.S. Department of Agriculture, N.R.C.S.S. *Java Newhall simulation model (jNSM)*, U.S. Department of Agriculture, Version 1.6.1., https://www.nrcs.usda.gov/wps/portal/nrcs/detail/soils/survey/class/?cid=nrcs142p2_053559, Accessed 25 Sept. 2019: 2016.
89. Vepraskas, M.J.; Sprecher, S.W. Overview of Aquic Conditions and Hydric Soils. In *Aquic conditions and hydric soils: The problem soils,*, Vepraskas, M.J., Sprecher, S.W., Eds. 1997; Vol. 50.
90. Gomez Diaz, J.D.; Monterroso, A.I.; Ruiz, P.; Lechuga, L.M.; Álvarez, A.C.C.; Asensio, C. Soil moisture regimes in Mexico in a global 1.5°C warming scenario. *International*

Journal of Climate Change Strategies and Management **2019**, *11*, 465-482, doi:10.1108/IJCCSM-08-2018-0062.
91. Weiss, A.D. *Topographic position and landforms analysis*; Poster, ESRI User Conference, San Diego, California: San Diego, CA, 2001; pp 1-1.
92. Homer, C.G.; Dewitz, J.A.; Yang, L.; Jin, S.; Danielson, P.; Xian, G.; Coulston, J.; Herold, N.D.; Wickham, J.D.; Megown, K. Completion of the 2011 National Land Cover Database for the conterminous United States representing a decade of land cover change information. *Photogrammetric Engineering & Remote Sensing* **2015**, *81*, 345-354, doi:10.14358/PERS.81.5.345.
93. Chambers, J.C.; Beck, J.L.; Campbell, S.; Carlson, J.; Christiansen, T.J.; Clause, K.J.; Dinkins, J.B.; Doherty, K.E.; Griffin, K.A.; Havlina, D.W., et al. Using resilience and resistance concepts to manage threats to sagebrush ecosystems, Gunnison sage-grouse, and greater sage-grouse in their eastern range: a strategic multi-scale approach. U.S. Department of Agriculture, Forest Service, Rocky Mountain Research Station: 2016; p 143.
94. Chambers, J.C.; Bradley, B.A.; Brown, C.S.; D'Antonio, C.; Germino, M.J.; Grace, J.B.; Hardegree, S.P.; Miller, R.F.; Pyke, D.a. Resilience to stress and disturbance, and resistance to Bromus tectorum L. invasion in cold desert shrublands of western North America. *Ecosystems* **2014**, *17*, 360-375, doi:10.1007/s10021-013-9725-5.
95. Chambers, J.C.; Brooks, M.L.; Germino, M.J.; Maestas, J.D.; Board, D.I.; Jones, M.O.; Allred, B.W. Operationalizing resilience and resistance concepts to address invasive grass-fire cycles. *Frontiers in Ecology and Evolution* **2019**, *7*, 1-25, doi:10.3389/fevo.2019.00185.
96. Chambers, J.C.; Miller, R.F.; Board, D.I.; Pyke, D.A.; Roundy, B.A.; Grace, J.B.; Schupp, E.W.; Tausch, R.J. Resilience and resistance of sagebrush ecosystems: implications for state and transition models and management treatments. *Rangeland Ecology and Management* **2014**, *67*, 440-454, doi:10.2111/REM-D-13-00074.1.
97. U.S. Department of Agriculture, N.R.C.S.S. *Soil data development toolbox*, U.S. Department of Agriculture, https://www.nrcs.usda.gov/wps/portal/nrcs/detail/soils/survey/office/ssr11/?cid=nrcseprd1327265, Accessed 17 Apr. 2021: 2021.